Alcom-FT Technical Report Series
ALCOMFT-TR-01-20

RANDOM MAPS, COALESCING SADDLES, SINGULARITY ANALYSIS, AND AIRY PHENOMENA

CYRIL BANDERIER, PHILIPPE FLAJOLET, GILLES SCHAEFFER, AND MICHÈLE SORIA

Abstract. A considerable number of asymptotic distributions arising in random combinatorics and analysis of algorithms are of the exponential-quadratic type, that is, Gaussian. We exhibit a class of "universal" phenomena that are of the exponential-cubic type, corresponding to distributions that involve the Airy function. In this paper, such Airy phenomena are related to the coalescence of saddle points and the confluence of singularities of generating functions. For about a dozen types of planar maps, a common Airy distribution (equivalently, a stable law of exponent 3/2) describes the sizes of cores and of largest (multi)connected components. Consequences include the analysis and fine optimization of random generation algorithms for multiply connected planar graphs, as well as the general classification of compositional schemas in analytic combinatorics.

Introduction

Maps are planar graphs embedded in the plane, and as such, they model the topology of many geometric arrangements in the plane and in low dimensions (*e.g.*, 3-dimensional convex polyhedra). This paper concerns itself with the statistical properties of random maps, *i.e.*, the question of what such a random map typically looks like. We focus here on connectivity issues, with the specific goal of finely characterizing the size of the highly connected "core" of a random map.

The bases of an enumerative theory of maps have been laid by Tutte [44] in the 1960's, this in an attempt to attack the four-colour conjecture. The present paper builds upon Tutte's results and upon previous analyses of largest components given by Bender, Richmond, Wormald, and Gao [7, 24]. We establish the common occurrence of an interesting probability distribution, the "Airy distribution of the map type", that precisely quantifies the sizes of cores in about a dozen varieties of maps, including general maps, triangulations, 2-connected maps, etc. As a corollary, we are able to improve on the complexity of the best known random samplers for multiply connected planar graphs and convex polyhedra from [40].

The analysis that we introduce is largely based on a method of "coalescing saddle points" that was perfected in the 1950's by applied mathematicians [3, 8, 47] and has found scattered applications in statistical physics and the study of phase transitions [37]. However, this method does not appear to have been employed so far in the field of random combinatorics. We claim some generality for the approach proposed here on at least two counts. First, a number of enumerative problems are known to be of the "Lagrangean type", being related to the Lagrange inversion theorem and its associated combinatorics. The classical saddle point method

Date: March 9, 2001.

is then instrumental in providing asymptotics of simpler problems. However, the confluence of saddle points that presents itself in "critical regions" is a stumbling block for the basic method. As we show here, planar maps are precisely instances of this situation. Next, parallel developments suggested by the theory of random maps and the corresponding integration contours lead to the precise analysis of a general composition schema. Indeed, it is known, in the realm of analytic combinatorics, that asymptotic properties of random structures are closely related to singular exponents of counting generating functions. For "most" recursive objects the exponent is $\frac{1}{2}$ and the probabilistic phenomena are described by classical laws, like Gaussian, exponential, or Poisson. Methods of the paper permit us to quantify distributions associated with singular exponents $\frac{3}{2}$ present in maps and unrooted trees, and, more generally, they extend to distributions occurring in relation to compositions of generating functions with algebraic-logarithmic singularities.

Very roughly, the classical saddle point method gives rise to probabilistic and asymptotic phenomena that are in the scale of $n^{1/2}$ and the analytic approximations are in the form of an "exponential-quadratic" (e^{-x^2}) corresponding to Gaussian laws. The coalescent saddle-point method presented here gives rise to phenomena in the scale of $n^{1/3}$, with analytic approximations of the "exponential-cubic type" (e^{ix^3}), which, as we shall explain, is conducive to Airy laws. The Airy phenomena that we uncover in random combinatorics should thus be expected to be of a fair degree of universality. Here are scattered occurrences of what we recognize as Airy phenomena in the perspective of this paper: the emergence of first cycles and of the giant component in the Erdős-Rényi graph model [18, 22, 29], the enumeration of random forests of unrooted trees [31], cluster formation in the construction of linear probing hashed tables [21, 30], the area under excursions and the cumulative storage cost of dynamically varying stacks [33], the area of certain polyominoes [14], path length in combinatorial tree models [42], and, perhaps, the threshold phenomena involved in the celebrated random 2-SAT problem [9]. We briefly return to these questions in the conclusion section of the paper.

Plan of the paper. Basics of maps are introduced in Section 1 where the Airy distribution is presented. The enumerative theory can be developed along two parallel lines, one Lagrangean, the other based on singularity analysis. We first approach the analysis of core size via the Lagrangean framework and variations of the saddle point method: a fine analysis of the geometry of associated complex curves is shown to open access to the size of the core, with the Airy distribution arising from double or "nearby" saddles (Section 2); a refined analysis based on the method of coalescent saddle points then enables us to quantify the distribution of core size over a wide range with precise large deviation estimates (Section 3). By singularity analysis techniques, we show more generally that the very same Airy law is bound to occur in any instance of a composition schema of singular type ($\frac{3}{2} \circ \frac{3}{2}$), which sheds a different light on the previous analyses; see Section 4. The methods based on saddle points and singularities are then applied to about a dozen types of planar maps, thereby providing a precise quantification of largest multiconnected components, with consequences on the random generation of highly connected planar graphs (Section 5). Finally, the singularity analysis methods can be extended to any composition schema that is "critical": see Appendix A where connections with stable distributions of probability theory are also discussed. Major

analytic properties of the Airy distribution "of the map type" are gathered in Appendix B. Here is a diagram summarizing the logical structure of the paper:

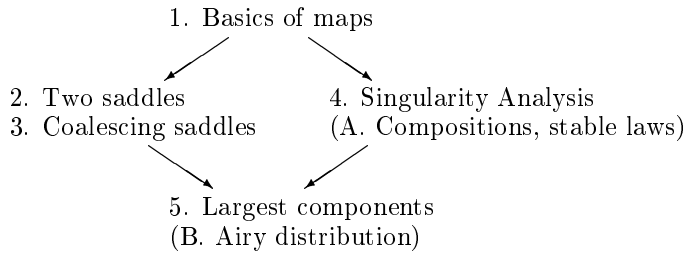

An extended abstract of this paper has been presented at the *ICALP'2000* conference; see [2].

1. Basics of maps

This section organizes known facts about the enumeration of maps for the convenience of readers not familiar with this chapter of combinatorial theory. It is intended as a preparation of the technical treatment in Sections 2–5 that rely on the Lagrangean framework (which provides exact power representations for map counts) and on singularity analysis (which provides direct asymptotic estimates).

A *map* is an embedding of a connected *planar* graph in the sphere, considered up to orientation preserving homeomorphisms. By construction the complement of the vertices and edges of a map in the sphere is a union of simply connected *faces*. In general loops and multiple edges are allowed. A map is completely characterized by its underlying graph together with a cyclical ordering of edges around each vertex. Following Tutte [43, 44], we consider *rooted* maps, that is, maps with an oriented edge called the *root*—this simplifies the analysis without essentially affecting statistical properties (see [38] and Section 5). In order to represent maps on the plane, a point of the sphere must be placed at infinity; by convention we always choose it so that the root runs along the infinite face counterclockwise. Figure 1 illustrate this convention. *From now on, unless explicitly mentioned, all maps are rooted.*

Generically, we take $\mathcal{M}$ and $\mathcal{C}$ to be two classes of maps, with $\mathcal{M}_n$, $\mathcal{C}_n$ the subsets of elements of size n (typically, elements with n edges). Here, $\mathcal{C}$ is always a subset of $\mathcal{M}$ that satisfies additional properties—typically, higher connectivity. The elements of $\mathcal{M}$ are then called the "basic maps" and the elements of $\mathcal{C}$ are called the "core-maps". We define informally the *core-size* of a map $\mathfrak{m} \in \mathcal{M}$ as the size of the largest $\mathcal{C}$–component of $\mathfrak{m}$ that contains the root of $\mathfrak{m}$.

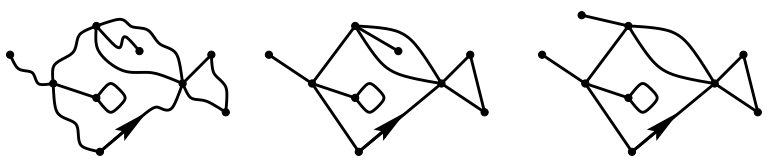

FIGURE 1. Three representations of maps. The first two are identical as maps, while the third one is not, although the three underlying planar graphs are identical.

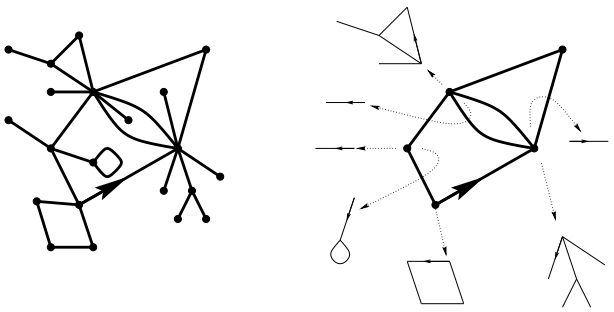

FIGURE 2. The decomposition of a map into its nonseparable core and the pending submaps.

As a pilot example, we shall specialize the basic maps $\mathcal{M}$ to be the class of all[1] maps with size taken as the number of edges. Define a *separating vertex* (or *articulation point*) as a vertex whose removal disconnects the graph. The class $\mathcal{C}_k$ will then be taken as the set of nonseparable maps with k edges, where a map is called *nonseparable* (or *2-connected*) if it has no separating vertex. In this case, the *core* of a map is obtained by starting from the root and removing all "pending" submaps that are attached only through an articulation point. This is illustrated by Figure 2, in which the central map on the right is a nonseparable map, namely the core of the map displayed on the left.

Our major objective is to characterize the probabilistic properties of core-size of a random element of $\mathcal{M}_n$, that is, of a random map of size n, when all elements are taken equally likely. Core-size then becomes a random variable X_n defined on $\mathcal{M}_n$. In essence, the pilot example thus deals with 2-connectivity in random (connected) maps. The paradigm that we illustrate by a particular example is in fact of considerable generality as can be seen from Section 5 below.

1.1. **The physics of maps.** From earlier works [7, 24, 39], it is known that a random map of $\mathcal{M}_n$ has with high probability a core that is either "very small" (roughly of size $k = O(1)$) or "very large" (being $\Theta(n)$). The probability distribution $\Pr(X_n = k)$ thus has two distinct modes. The small region (say $k = o(n)$) has been well quantified by previous authors, see [7, 24, 39]: a fraction $p_s = \frac{2}{3}$ of the probability mass is concentrated there. The large region is also known from these authors to have probability mass $p_\ell = 1 - p_s = \frac{1}{3}$ concentrated around $\alpha_0 n$ with $\alpha_0 = \frac{1}{3}$ but this region has been much less explored as it poses specific analytical difficulties. Our results precisely characterize what happens in terms of an Airy distribution.

The Airy function $\mathrm{Ai}(z)$, as introduced by the Royal Astronomer Sir George Bidell Airy, is a solution of the equation $y'' - zy = 0$ that can be defined by a

[1]We also speak of the class of "general" maps when we need to contrast it with special classes of maps.

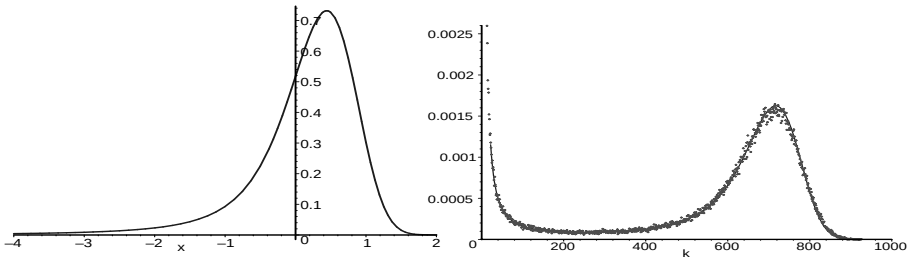

FIGURE 3. Left: The standard Airy distribution. Right: Observed frequencies of core-sizes $k \in [20; 1000]$ in 50,000 random maps of size 2,000, showing the bimodal character of the distribution.

variety of integral or power series representations including (see [1, 45]):

$$\begin{aligned} \mathrm{Ai}(z) &= \frac{1}{2\pi}\int_{-\infty}^{+\infty} e^{i(zt+t^3/3)}\,dt \\ &= \frac{1}{\pi 3^{2/3}}\sum_{n=0}^{\infty}\left(3^{1/3}z\right)^n \frac{\Gamma((n+1)/3)}{n!}\sin\frac{2(n+1)\pi}{3}\,. \end{aligned} \tag{1}$$

Equipped with this definition, we present the main character of the paper, a probability distribution closely related to the Airy function.

Definition 1. *The standard Airy distribution (of the "map type") is the probability distribution whose density is*

$$\begin{aligned} \mathcal{A}(x) &= 2e^{-2x^3/3}\left(x\mathrm{Ai}(x^2) - \mathrm{Ai}'(x^2)\right) \\ &= \frac{1}{\pi x}\sum_{n\geqslant 1}(-x3^{2/3})^n \frac{\Gamma(2n/3+1)}{n!}\sin(-2n\pi/3). \end{aligned} \tag{2}$$

The Airy distribution of parameter c is defined by the density $c\mathcal{A}(cx)$.

Major properties of the function $\mathcal{A}(x)$ (including the equivalence between the two definitions of (2)) are gathered in Appendix B. The Airy distribution[2] is a probability distribution, *i.e.*, $\int_{\mathbb{R}}\mathcal{A}(x)\,dx = 1$, and an unusual feature is the fact that the tails are extremely asymmetric:

$$\mathcal{A}(x) \underset{x\to-\infty}{\sim} \frac{1}{4\sqrt{\pi}}|x|^{-5/2} \quad \text{and} \quad \mathcal{A}(x) \underset{x\to\infty}{\sim} \frac{2}{\sqrt{\pi}}\,x^{1/2}\exp\left(-\frac{4}{3}x^3\right). \tag{3}$$

A plot of the map–Airy distribution is presented in Figure 3 (left).

We shall find that the size of the core (when conditioned upon the large region) and the size of the largest 2-connected component of a random map are described asymptotically by an Airy law of this type. Figure 3 (right) exemplifies this with simulation results of core size: the "bimodal" character of the combinatorial distribution is clearly visible and the convergence of simulation data to the limit Airy distribution curve is already excellent at size $n = 2,000$. (Additional simulation data are given in Section 5.4.)

[2]The Airy distribution of the map type is known in the probability literature as a stable law of index $\frac{3}{2}$ (see Appendix A), and in celestial mechanics as the Holtsmark distribution.

1.2. **The combinatorics of maps.** Let M_n and C_k be the cardinalities of $\mathcal{M}_n$ and $\mathcal{C}_k$. The *generating functions* of $\mathcal{M}$ and $\mathcal{C}$ are respectively defined by

$$M(z) := \sum_{n\geqslant 1} M_n z^n \qquad \text{and} \qquad C(z) := \sum_{k\geqslant 1} C_k z^k.$$

Root-face decompositions. As shown by Tutte, there results from a root-face decomposition and from the quadratic method [26, Sec. 2.9] that many families of maps have a generating function $M(z)$ that is algebraic, and more specifically *Lagrangean*, which means that it can be parametrized by a system of the form

$$M(z) = \Psi(L(z)) \quad \text{where} \quad L(z) = z\phi(L(z)), \tag{4}$$

for two rational power series Ψ, ϕ, with L being determined implicitly by ϕ. We first prove that $M(z)$ is Lagrangean.

Proposition 1. *The generating function of general maps $M(z)$ is Lagrangean:*

$$\begin{aligned} M(z) &= \Psi(L(z)), \qquad & L(z) &= z\phi(L(z)) \\ \Psi(y) &= \frac{1}{3}y(2-y), \qquad & \phi(y) &= 3(1+y)^2. \end{aligned} \tag{5}$$

Accordingly, the number of general maps satisfies

$$M_n \equiv [z^n]M(z) = \frac{2\cdot 3^n\,(2n)!}{(n+2)!\,n!} \tag{6}$$

Proof (sketch). Schematically, for the family of general maps with n edges, the treatment goes as follows. Let $M^\diamond(z,u)$ be the bivariate generating function of maps where z, u mark respectively the number of edges and the degree of the root face. Also the map of size 0 with one vertex and no edge is momentarily allowed. (Consequently, $M(z) = M^\diamond(z,1) - 1$.) First, the functional equation

$$M^\diamond(z,u) = 1 + u^2 z M^\diamond(z,u)^2 + uz\frac{M^\diamond(z,1) - uM^\diamond(z,u)}{1-u} \tag{7}$$

reflects the construction of maps starting from the map of size 0 by either adding an isthmus (also known as bridge) that connects two simpler maps, or by adding an edge that cuts across an existing face. From (7), upon isolating $M^\diamond(z,u)$, one gets the equivalent "quadratic form"

$$\left(M^\diamond(z,u) - R(z,u)\right)^2 = Q(z,u) + \frac{M^\diamond(z,1)}{u(1-u)}, \tag{8}$$

for some explicit rational functions $Q(z,u)$ and $R(z,u)$. The principle of the quadratic method is to bind z and u in such a way (*a priori* unknown) that the left hand side vanishes. Consequently, under the binding, the right side of (8) should have a double root, which is expressed by the conditions

$$\left(Q(z,u) + \frac{M^\diamond(z,1)}{u(1-u)}\right) = 0, \quad \frac{\partial}{\partial u}\left(Q(z,u) + \frac{M^\diamond(z,1)}{u(1-u)}\right) = 0.$$

The compatibility condition of these two equations is then expressed by two rational relations between the three quantities $M^\diamond(z,1)$, u, and z, from which one finds that $u = u(z)$ should satisfy $u^2 z + (u-1)(2u-3) = 0$. Computations based on the further change of parameter $L = 1/(1-u)$ (see [26, 43] and Section 5 for other examples) then lead to the Lagrangean parametrization (5).

There results from the form (4) and from the Lagrange inversion theorem [26] an explicit form for the coefficients of $M(z)$, namely,

$$M_n \equiv [z^n]M(z) = \frac{1}{n}[y^{n-1}]\Psi'(y)\phi(y)^n, \tag{9}$$

where $[z^n]F(z)$ denotes the coefficient of z^n in the series expansion of $F(z)$. For the family of general maps, this instantiates to (6) as given in the statement of the theorem. □

Alternatively, elimination shows that $M(z)$ is an algebraic function, in this case admitting of closed form:

$$M(z) = -1 + \frac{1}{54z^2}\left(-(1-18z) + (1-12z)^{3/2}\right). \tag{10}$$

Substitution decompositions. As shown again by Tutte, maps satisfy additionally relations of the "substitution type". Such relations usually take the form $\mathcal{M} = \mathcal{C} \circ \mathcal{H}$ where the family $\mathcal{H}$ is a simple variation of the "basic" family $\mathcal{M}$ while the "core" family $\mathcal{C}$ is defined by stronger connectivity constraints.

Proposition 2. *The generating function of nonseparable maps is Lagrangean:*

$$\begin{aligned} C(t) &= \Psi(\widetilde{L}(t)), & \widetilde{L}(t) &= t\,\widetilde{\phi}(\widetilde{L}(t)) \\ \Psi(y) &= \frac{1}{3}y(2-y), & \widetilde{\phi}(y) &= \frac{3}{(1-y/3)^2}. \end{aligned} \tag{11}$$

Accordingly, the number of nonseparable maps satisfies

$$C_k \equiv [z^k]C(z) = \frac{4(3k-3)!}{(2k)!\,(k-1)!}. \tag{12}$$

Proof (sketch). Between the family $\mathcal{M}$ of general maps and the family $\mathcal{C}$ of nonseparable maps, the substitution relation

$$M(z) = \sum_{k\geq 1} C_k z^k (1+M(z))^{2k} = C(H(z)), \quad \text{with} \quad H(z) = z(1+M(z))^2, \tag{13}$$

expresses that each map is formed of a *core* with k edges (chosen among the C_k nonseparable maps with k edges) in which $2k$ (possibly empty) maps are substituted. This is exactly the decomposition illustrated by Figure 2: the core is obtained starting from the root edge[3] by detaching all pending submaps until there is no separation vertex left; conversely a submap can be attached at each of the $2k$ "corners" of a nonseparable map in order to form a general map.

An equation like (13) determines effectively (albeit in an implicit manner) the exact enumeration of objects of type $\mathcal{C}$ which are more "complex", *i.e.*, here, more highly connected than the initial maps of $\mathcal{M}$. One can go further. In view of Equations (4), (13), the generating function $H(z)$ is also expressible in terms of the basic Lagrangean series $L(z)$:

$$H(z) = \psi(L(z)) \quad \text{with} \quad \psi(y) = \frac{y}{3}\left(1-\frac{y}{3}\right)^2. \tag{14}$$

In order to extract the generating function $C(t)$ from the relation $M(z) = C(H(z))$, it is natural to introduce the change of variables $z = z(t)$ defined by $t = H(z)$, which

[3]Remark that this decomposition covers the cases when the root is a bridge or a loop, provided one adopts the convention that the two maps with one edge (*i.e.*, the bridge and the loop) are nonseparable.

yields $C(t) = M(z(t))$. As both $M(z)$ and $H(z)$ are defined in terms of $L(z)$, letting $\widetilde{L}(t) = L(z(t))$ leads to the system (11). This parametrization is finally amenable to the Lagrange inversion theorem, hence the expression (12) for the coefficients C_k. □

The proof also shows that the generating function $C(t)$ of nonseparable maps is a cubic algebraic function,

$$C^3 + 2C^2 + (1 - 18t)C + 27t^2 - 2t = 0,$$

that is an elementary variant of the generating function of ternary trees.

The core-size parameter. Our analysis assumes the *uniform distribution* over general maps of size n, with each map being taken with probability $1/M_n$. Under this model, we let X_n denote the random variable of core-size. Let $\mathcal{M}_{n,k}$ be the set of maps with n edges whose core comprises k edges; we define the *bivariate generating function*

$$M(z,u) = \sum_{n,k} M_{n,k} u^k z^n \quad \text{with } M_{n,k} = \text{card}\,(\mathcal{M}_{n,k}).$$

The following obvious refinement of (13) gives access to core-size:

$$M(z,u) = C(uH(z)) \quad (\text{with } H(z) = z(1 + M(z))^2). \tag{15}$$

In summary:

Proposition 3. *The* probability distribution of core-size *is determined by*

$$\Pr(X_n = k) = \frac{C_k}{M_n}\,[z^n]H(z)^k, \tag{16}$$

where one has, with $\phi(y) = 3(1+y)^2$ *and* $\psi(y) = (y/3)(1 - y/3)^2$*:*

$$[z^n]H(z)^k = \frac{k}{n}[y^{n-1}]\psi'(y)\psi(y)^{k-1}\phi(y)^n. \tag{17}$$

Proof. Relation (16) is a mere rephrasing of (15). The expression (17) results from (14) and Lagrange inversion. □

The involved generating functions are algebraic (and even rationally parametrized under the Lagrangean framework), which leads to complicated alternating binomial sums expressing $\Pr(X_n = k)$. The exponential cancellations involved are however not tractable in this elementary way, and complex asymptotic methods must be resorted to.

1.3. **The asymptotics of maps.** There is another side to the coin, to be explored further in Section 4. It relies on singularity analysis [20], the principle being a general correspondence between the expansion of a generating function at a singularity and the asymptotic form of its coefficients.

Proposition 4. *Each generating function* $M(z), C(z), H(z)$ *has a unique dominant singularity (at* $\frac{1}{12}, \frac{4}{27}, \frac{1}{12}$ *resp.) and a singular expansion with singular exponent* $\frac{3}{2}$ *at its singularity in the sense that*

$$\begin{cases} M(z) &= \frac{1}{3} - \frac{4}{3}(1-12z) + \frac{8}{3}(1-12z)^{3/2} + O((1-12z)^2) \\ H(z) &= \frac{4}{27} - \frac{4}{9}(1-12z) + \frac{16}{27}(1-12z)^{3/2} + O((1-12z)^2) \\ C(z) &= \frac{1}{3} - \frac{4}{9}(1-27z/4) + \frac{8\sqrt{3}}{81}(1-27z/4)^{3/2} + O((1-27z/4)^2). \end{cases} \tag{18}$$

In particular, one has

$$M_n \sim \frac{2}{\sqrt{\pi}} 12^n n^{-5/2}, \quad \text{and} \quad C_k \sim \frac{2}{27}\sqrt{\frac{3}{\pi}}\left(\frac{27}{4}\right)^k k^{-5/2}. \tag{19}$$

Proof (sketch). In this proof, we purposely conduct the discussion in abstract terms, and relate the existence of such expansions to the general Lagrangean framework. The motivation stems from the need to cover the schemas of Section 5. (Clearly, singular expansions of M, C, H could be derived by direct computation while the asymptotic forms of (19) are obvious consequences of the closed-forms available for M_n, C_k in this particular instance.)

(*i*) *The universal asymptotics of maps.* An implicitly defined function $L(z) = z\phi(L(z))$ has in general an isolated singularity of the square-root type dictated by a failure of the implicit function theorem [5, 34]:

$$L(z) = \tau - l_{1/2}(1 - z/\rho)^{1/2} + O(1 - z/\rho) \qquad (l_{1/2} > 0); \tag{20}$$

there the singularity ρ and the singular value τ are determined by the equations

$$\tau\phi'(\tau) - \phi(\tau) = 0, \qquad \rho = \frac{\tau}{\phi(\tau)}. \tag{21}$$

The expansion (20) yields in turn the singular expansion of the generating function of maps via $M(z) = \Psi(L(z))$. It appears that in all known map-related parametrizations of the form (4), the cancellation $\Psi'(\tau) = 0$ holds, so that the singular exponent is shifted to $3/2$:

$$M(z) = \Psi(L(z)) = \Psi(\tau) - m_1(1 - z/\rho) + m_{3/2}(1 - z/\rho)^{3/2} + O((1 - z/\rho)^2). \tag{22}$$

(The constants $l_{1/2}, m_1, m_{3/2}$ are positive and computable from ϕ, Ψ, τ.) According to singularity analysis [20] (or the Darboux-Pólya method [5]), the singular expansion then entails

$$M_n \sim \frac{3m_{3/2}}{4\sqrt{\pi}} \frac{\rho^{-n}}{n^{5/2}}. \tag{23}$$

This generic asymptotic form is "universal" in so far as it is valid for all known "natural" families of maps (see Section 5 and the discussion in [6]).

(*ii*) *Substitution relations and asymptotics.* The substitution relation (13) entails another remarkable property of the asymptotic expansions of $M(z)$, $H(z)$ and $C(z)$. First, as H is defined in terms of M by $H(z) = z(1 + M(z))^2$, both H and M have the same dominant singularity, ρ, with singular exponent $3/2$. In particular, one has

$$H(z) = \psi(L(z)) = \psi(\tau) - h_1(1 - z/\rho) + h_{3/2}(1 - z/\rho)^{3/2} + O((1 - z/\rho)^2). \tag{24}$$

and, accordingly, the parametrization $H(z) = \psi(L(z))$ must also satisfy $\psi'(\tau) = 0$.

The function $\widetilde{L}$ that determines C is implicitly defined, so that its singularity $\widetilde{\rho}$ and singular value $\widetilde{\tau}$ are solutions of a system analogous to (21), which reduces to $\psi'(\widetilde{\tau}) = 0$, $\widetilde{\rho} = \psi(\widetilde{\tau})$. Accordingly, one has $\widetilde{\tau} = \tau$, hence $\widetilde{\rho} = \psi(\tau)$, and

$$C(t) = \Psi(\tau) - c_1(1 - t/\psi(\tau)) + c_{3/2}(1 - t/\psi(\tau))^{3/2} + O((1 - t/\psi(\tau))^2), \tag{25}$$

where c_1 and $c_{3/2}$ are computable positive numbers. This results in

$$C_k = [z^k]C(z) \sim \frac{3c_{3/2}}{4\sqrt{\pi}} \frac{\psi(\tau)^{-k}}{k^{5/2}}. \tag{26}$$

The analysis specializes for the families of general maps and nonseparable maps where it provides $\tau = 1,\ \rho = \frac{1}{12},\ \psi(\tau) = \frac{4}{27}$. Hence, the singular expansions of (18) and the asymptotic forms (19) of the exact counts (6) and (12). □

Propositions 3 and 4 open access to the distribution of core-size in two parallel ways.

(*i*) The structure constant τ which is by construction a saddle point of $\phi(z)/z$ plays a fundamental rôle, and from the preceding proof one has the "coalescence relations"

$$\frac{d}{dz}\left(\frac{\phi(z)}{z}\right)_{z=\tau} = 0, \qquad \frac{d}{dz}\left(\psi(z)\right)_{z=\tau} = 0. \tag{27}$$

The coalescence relations express the fact that τ is a saddle point common to $\phi(z)/z$ and $\psi(z)$. The saddle point analysis of Sections 2–3 takes off from the power forms (16), (17) provided by the Lagrangean framework and from the relations (27) which can be taken as basic axioms.

(*ii*) In terms of the composition equation $M(z) = C(H(z))$, the calculation above implies that the value of $H(z)$ at its singularity ρ coincides with the dominant singularity of $C(z)$:

$$H(\rho) = \text{r.o.c}\,(C(z)), \tag{28}$$

where "r.o.c." denotes radius of convergence. Such a composition $\mathcal{C} \circ \mathcal{H}$ is called *critical*. This situation of confluence of singularities is considered in full generality in Section 4 where the analysis of core size is developed from the power form (16) of Proposition 3 and from the criticality assumption (28).

Both approaches are "universal" for cores in map. Section 5 lists several other types of maps for which the coalescence relations (27) hold (with various rational function pairs ϕ, ψ), and for which core-size is described by a composition schema that is critical in the sense of (28) (with various algebraic functions C, M).

2. Two saddles

The probability distribution of core-size in maps is determined by Proposition 3 above. What is essentially needed is a way to estimate $[z^n]H(z)^k$. The saddle point approach starts from a contour integral representation based on the Lagrangean form, Equation (17), in conjunction with Cauchy's coefficient formula,

$$\begin{aligned}[z^n]H^k(z) &= \frac{k}{n}\frac{1}{2i\pi}\int_\Gamma z\psi(z)'\psi(z)^{k-1}\phi(z)^n\frac{dz}{z^{n+1}} \\ &= \frac{k}{n}\frac{1}{2i\pi}\int_\Gamma G(z)\,\exp(nK(z))\,dz\end{aligned} \tag{29}$$

There Γ is a contour encircling the origin anticlockwise, while

$$K(z) \equiv K(z;n,k) = \frac{k}{n}\log\psi(z) + \log(\phi(z)/z), \quad \text{and} \quad G(z) = \frac{\psi'(z)}{\psi(z)} \tag{30}$$

are respectively the "kernel" and the "cofactor" of the integrand.

In simpler cases, integrals over complex contours involving large powers are amenable to the basic saddle point method. The idea consists in deforming the contour Γ in the complex plane, this, in order to have it cross a saddle point of the integrand, (*i.e.*, a zero of the derivative) and to take advantage of concentration of the integral near the saddle point. Then local expansions yield approximations that

are of the "exponential quadratic" type when the saddle point is simple (*i.e.*, only the first derivative vanishes). We refer to de Bruijn's book for a vivid description of standard saddle point landscapes in connection with asymptotic analysis [12].

For the problem at hand, there are two real saddle points, given by the saddle point equation $\frac{\partial}{\partial z}K(z) = 0$, one is *fixed* and equal to τ, while the other varies with n, k. In particular, for nonseparable cores of general maps, one has

$$\tau = 1 \quad \text{and} \quad \tau' = 3\frac{n-k}{n+3k}. \tag{31}$$

The relative positions of these two saddle points and the geometry of the integrand evolve with the ratio k/n, as shown by Figure 4. The basic saddle point

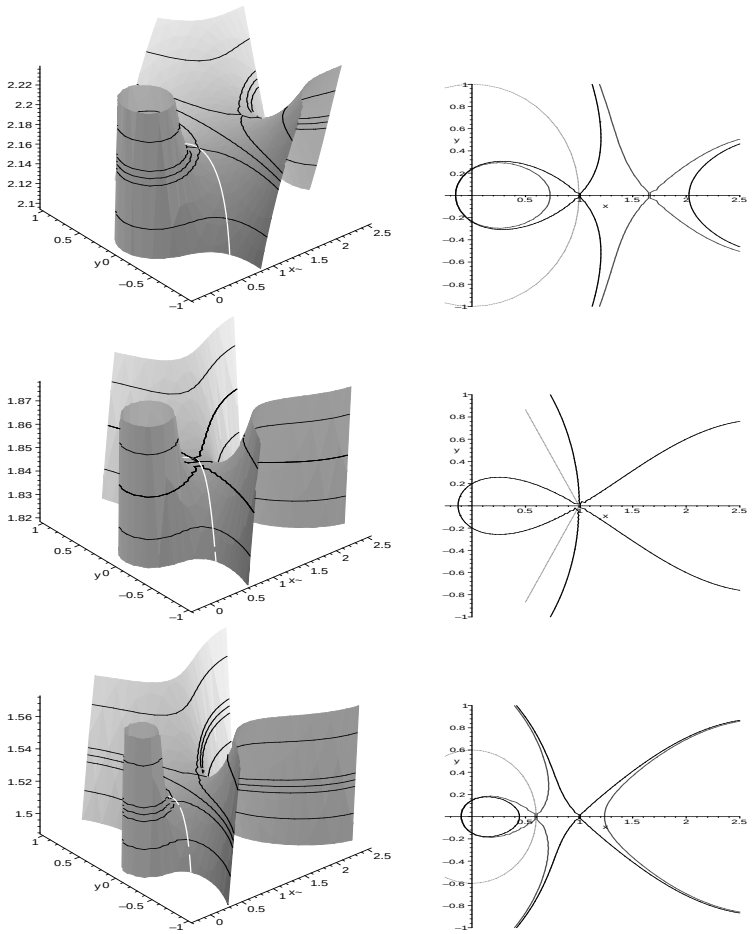

FIGURE 4. Saddle landscapes and paths of integrations. From top to bottom, $k = \alpha n$ with $\alpha = 1/6$, $\alpha = 1/3$, and $\alpha = 1/2$. The path of integration (dotted line) is seen to go through the dominant saddle which is double in the middle landscape and simple in the other two. Dark and soft gray lines are respectively the level curves $\Re(K(\tau))$ and $\Re(K(\tau'))$ of the kernel $K(z) = \alpha \log \psi + \log(\phi/z)$.

k:	Left tail $[\epsilon n, (\alpha_0 - \epsilon)n]$	Centre $\alpha_0 n$	Right Tail $[(\alpha_0 + \epsilon)n, (1-\epsilon)n]$
Saddle points:	$\tau < \tau'$	$\tau = \tau'$	$\tau > \tau'$
Method:	simple saddle point (Section 2.1)	double saddle point (Section 2.2)	simple saddle point (Section 2.1)
Type:	$\int e^{-t^2} dt$	$\int t e^{-t^3} dt$	$\int e^{-t^2} dt$
Angle:	$\pm\frac{\pi}{2}$	$\pm\frac{2\pi}{3}$	$\pm\frac{\pi}{2}$
Error:	$n^{-1/2}$	$n^{-1/3+\epsilon}$	$n^{-1/2}$

k:	Central region $[\alpha_0 n + a n^{2/3}, \alpha_0 n + b n^{2/3}]$	"Wide" region $[\epsilon n, (1-\epsilon)n]$
Saddle points:	$\tau' \approx \tau$	
Method:	nearby saddle points (Section 2.3)	coalescing saddle points (Section 3)
Type:	$\int (x-t) e^{\,xt - t^3/3} dt$	$\int (x-t) e^{\,xt - t^3/3} dt$
Angle:	$\pm\frac{2\pi}{3}$	$\to$ cubic curve
Error:	$n^{-1/3+\epsilon}$	$n^{-1/3}$

FIGURE 5. Top: A broad classification of the methods involved in the classification of tails and centre of the core-size distribution. Bottom: Refinements of the saddle point method applicable to the critical region of the law of core-size.

method applies when these two points are sufficiently separated from one another, that is, as long as $\alpha := k/n$ is "far away" from the special value $\alpha_0 \equiv \frac{1}{3}$. This corresponds to the situation already known from the works [7, 24, 39]. The situation changes and there appears a "critical" region when k assumes values near $\alpha_0 n$ (as it turns out, in the scale of $n^{2/3}$). In that interesting case, the basic version of the saddle point method ceases to be applicable, and this is precisely where we fit in: by a detailed examination of the analytic geometry of the saddle points, we provide suitable integration contours that "capture" the main asymptotic contributions. Such an approach leads to a precise quantification of core-size in random maps. Figure 5 summarizes the main methods involved in the saddle-point analyses of this and the next section.

2.1. **Distinct saddles.** When k is far enough from $\alpha_0 n$, one of the two saddle points is nearer to the origin and predominates. In that case, the basic method applies, with the integration contour a circle centred at the origin and passing through the dominant saddle point. This corresponds to the already known results of Bender, Gao, Richmond, and Wormald [7, 24] supplemented by [39].

Theorem 1 (Tails and distinct saddles [24])**.** *Consider nonseparable cores of general maps. Let $\alpha = k/n$, $\alpha_0 \equiv 1/3$, and take ϵ an arbitrarily small positive number.*

(i) The left tail of the probability distribution of core-size has a polynomial decay: uniformly for $\epsilon n < k < (\alpha_0 - \epsilon)n$, one has

$$\Pr(X_n = k) \sim \frac{1}{3^5\sqrt{\pi}} \frac{1}{k^{3/2}(\alpha_0 - \alpha)^{5/2}}.$$

(*ii*) *The right tail has an exponential decay: there exists a positive constant* $A < 1$ *such that, uniformly for* $(\alpha_0 + \epsilon)n < k < n(1-\epsilon)$, *one has*

$$\Pr(X_n = k) = O(A^n).$$

Proof (Sketch). We limit ourselves to brief indications on proof techniques (that rely on [7]), this merely to serve as a basis for comparison with the next sections. For both left and right tails, Γ is taken to be a circle through the saddle point that is "dominant" (in the sense that it is nearer to the origin). We denote by τ_d this dominant saddle point.

The main contribution to the integral arises from an immediate vicinity of τ_d. In this vicinity the kernel admits an expansion of the quadratic type

$$K(\tau_d + u) = K(\tau_d) - \kappa_2 \left|\alpha - \alpha_0\right| u^2 + O(u^3),$$

where κ_2 is a positive continuous function of α. In particular, provided α is far enough from α_0 the basic saddle point applies and the integral (29) is, up to lower order terms, given by the integral over a small vertical segment following the steepest descent line on both sides of τ_d. This yields

$$[z^n]H(z)^k \sim \frac{k}{n}\frac{\exp(K(\tau_d))^n}{2\pi}\int_{-\delta}^{\delta} G(\tau_d + u)\exp(-n\kappa_2\left|\alpha - \alpha_0\right| u^2 + O(nu^3))du,$$

where the "range" δ is chosen so that

$$n\delta^2 \to \infty, \qquad n\delta^3 \to 0,$$

ensuring a complete local capture of the contribution as well as validity of the quadratic approximation. Here, we adopt $\delta = \log n/\sqrt{n}$.

The left tail ($k < \alpha_0 n$) corresponds to $\tau_d = \tau$, *i.e.*, the fixed saddle point τ is dominant (Fig. 4, top). In this case the expansion of $G(\tau + u)$ leads to part (*i*) of the theorem. Remark that the slow decay of probabilities ($k^{-3/2}$) in this region results from the formula

$$\Pr(X_n = k) = \frac{C_k[z^n]H(z)^k}{M_n}$$

where the exponential rate of growth of $[z^n]H(z)^k$, namely $\exp(K(\tau))^n = \rho^{-n}\psi(\tau)^k$, exactly compensates the exponential rate of decay of C_k/M_n.

The right tail ($k > \alpha_0 n$) has $\tau_d = \tau'$ dominating; (Fig. 4, bottom). This case leads to part (*ii*) of the theorem and the exponential decay of probabilities follows because $K(\tau') < K(\tau)$ does not allow $\exp(K(\tau'))^n$ to catch up with the exponential factor present in C_k/M_n. □

The saddle point method can lead in fact to precise estimates with correction terms to any order, as long as α stays away from α_0. For instance, one has for the right tail: *there exist two real functions* $f(\alpha)$ *and* $g(\alpha)$, *positive and continuous on the interval* $[1/3, 1]$, *such that*

$$\Pr(X_n = k) \sim \frac{(\alpha - \alpha_0)^{1/2}}{(1-\alpha)^{3/2}} f(\alpha)\, n^{-1/2} e^{-n(\alpha-\alpha_0)^3\, g(\alpha)},$$

uniformly for $\alpha_0 n + n^{2/3}\lambda(n) < k < n - n^{2/3}\lambda(n)$, *where* $\lambda(n)$ *is any function tending to infinity.*

2.2. **A double saddle.** We next analyse the "centre" of the distribution, that is, consider the case where $k = \alpha_0 n$ exactly. Then, the two saddle points of (31) become equal: $\tau' = \tau$. This case serves to introduce with minimal apparatus the enhancements that need to be brought to the basic saddle point method. Observe that the complete confluence of the saddle points precludes the use of "exponential-quadratic" approximations and the problem becomes of an "exponential cubic" type. The following statement is a variant, with error terms added, of Theorem 1, case (c), by Bender, Richmond, and Wormald [7]. (See also comments after the proof.)

Theorem 2 (Centre and a double saddle)**.** *The centre of the probability distribution of the (nonseparable) core-size of a random element of $\mathcal{M}_n$ (general maps) satisfies, when $k = \alpha_0 n$ with $\alpha_0 = \frac{1}{3}$:*

$$\Pr(X_n = k) \sim \frac{3\sqrt{3}\,2^{2/3}\Gamma(2/3)}{8\pi} k^{-2/3} \left(1 + O(n^{-1/3}(\log n)^4)\right) . \approx .44441\, k^{-2/3} .$$

Proof. We present the proof in the form of a general discussion of kernel (30), in the case of a double saddle point at τ when $k = \alpha_0 n$. In this way, generic formulæ like (34) below can be later reused for all families of maps listed in the Section 5. (For the case of nonseparable cores of general maps, one should take $\alpha_0 = \frac{1}{3}$ and $\tau = 1$.)

When $k = \alpha_0 n$, Equation (29) becomes

$$[z^n]H^k(z) = \frac{\alpha_0}{2i\pi} \int_\Gamma G(z) \exp\left(nK(z)\right) dz, \tag{32}$$

where the kernel K reduces to $K(z) := \log\left((\phi/z)\psi^{\alpha_0}\right)$. By assumption, the quantity e^K has a double saddle point at τ sometimes called a "monkey saddle", *viz.*, a saddle with places for two legs *and* a tail. The idea consists in choosing a contour that is no longer a circle centred at the origin, but, rather, approaches the real axis at an angle (see Fig. 4, middle).

Global analysis. Let δ° be a small enough but fixed positive quantity (here, $\delta^\circ = 1/10$ proves adequate). Specifically, the integration path Γ consists of the following parts: (i) two (small) segments $\Delta_1^\circ, \Delta_2^\circ$ that have length δ° and intersect at τ, at an angle of $\pm 2\pi/3$; (ii) the part Γ° of a circle centred at 0 from which a small arc is taken out, joining with the nonreal ends of $\Delta_1^\circ, \Delta_2^\circ$.

By having chosen δ° small enough, we ensure that e^K decreases strictly in modulus along $\Delta_1^\circ, \Delta_2^\circ$, when going away from τ. By examining the global topography of the real part of $K(z)$ along Γ° (and possibly deforming the contour but keeping it homotopic to Γ° in $\mathbb{C}\setminus\{0\}$ for more complicated cases), we ensure that the modulus of the function e^K remains smaller than its value at the nonreal ends of $\Delta_0^\circ, \Delta_1^\circ$. Consequently, the contribution of the part due to Γ° is exponentially small.

Next, we shall choose a value $\delta < \delta^\circ$ (the "range") depending on n and tending to 0 as $n \to \infty$. With a suitable choice of δ, see (33) below, and by virtue of the decay of $|e^K|$ along the part of the contour at a distance from τ that is larger than δ, the corresponding contribution is also exponentially negligible (roughly like $\exp(-\log^3 n)$). Then, the analysis reduces to a purely local analysis of e^K. We denote by Δ_1, Δ_2 the parts of the contour that are at distance at most δ from τ and adopt a value of δ satisfying two conflicting requirements,

$$n\delta^3 \to \infty, \qquad n\delta^4 \to 0, \quad \text{specifically} \quad \delta = (\log n) n^{-1/3}. \tag{33}$$

Local analysis. We can now switch to the local analysis. The situation is such that there is coincidence of two saddle points (τ, τ'). Accordingly, the kernel K has a double saddle point in τ, meaning that its local expansion is of the cubic type:

$$K(z) = \kappa_0 - \kappa_3(z-\tau)^3 + O((z-\tau)^4) \qquad (\kappa_0, \kappa_3 > 0).$$

This cubic form together with the fact that κ_3 is positive explains the geometry of the "landscape" corresponding to $\left|e^K\right|$, in particular, the level curves, the steepest descent lines, and the steepest ascent lines [12]. For example, the steepest descent lines are at angles $0, 2\pi/3, -2\pi/3$ (see Figure 4). Thus, locally at τ, the integration path Γ follows two steepest descent lines of the landscape.

The contribution $I_{1,2}$ along $\Delta_1 \cup \Delta_2$ to the integral in (32) provides the dominant contribution and is estimated next by a local analysis of K for values of z near τ. Set $u = z - \tau$. The condition $n\delta^4 \to 0$ in (33) implies that terms of order 4 and higher do not matter asymptotically, and a simple calculation, using the fact that $G(\tau + u) = -g_1 u + O(u^2)$, yields

$$I_{1,2} := \int_{\Delta_1 \cup \Delta_2} G \cdot \exp(nK)\, dz = -g_1 \exp(\kappa_0)^n \int_{\Delta_1 \cup \Delta_2} u \exp\left(-n\kappa_3 u^3\right) (1 + O(n\delta^4))\, du\,.$$

The rightmost integral taken along $\Delta_1 \cup \Delta_2$ can be extended to two full half lines of angle $\pm 2\pi/3$ emanating from the origin, this at the expense of introducing only exponentially small error terms (since $n\delta^3 \to \infty$). The rescaling $v = u(n\kappa_3)^{1/3} \exp(2i\pi/3)$ on Δ_1 and $v = u(n\kappa_3)^{1/3} \exp(-2i\pi/3)$ on Δ_2 then shows that the completed integral equals

$$(n\kappa_3)^{-2/3}(e^{4i\pi/3} - e^{-4i\pi/3}) \int_0^{+\infty} v \exp(-v^3) dv = -(n\kappa_3)^{-2/3} \frac{i}{\sqrt{3}} \Gamma(2/3),$$

where the evaluation results from a cubic change of variable. In summary, we have found, with I_0 the (negligible) contribution due to the part $\Gamma \setminus (\Delta_1 \cup \Delta_2)$ of the contour,

$$[z^n] H^k(z) = \frac{\alpha_0}{2i\pi} (I_0 + I_{1,2}) = \frac{g_1}{\kappa_3^{2/3}} \frac{\Gamma(2/3)}{2\pi\sqrt{3}} \frac{\exp(\kappa_0)^n}{n^{2/3}} \left(1 + O(n\delta^4)\right).$$

The definition of the kernel K implies that g_1, κ_0 and κ_3 are expressible in terms of ϕ, ψ, and τ alone,

$$g_1 = \frac{\psi''(\tau)}{\psi(\tau)}, \quad \kappa_0 = \log\left(\frac{\phi(\tau)}{\tau} \psi^{\alpha_0}(\tau)\right), \quad \kappa_3 = 6\left(\frac{d^3}{dz^3} \frac{\phi(z)}{z} \psi_0^{\alpha}(z)\right)_{z=\tau},$$

which leads to

$$[z^n] H^k(z) = \frac{g_1}{\kappa_3^{2/3}} \frac{\Gamma(2/3)}{2\pi\sqrt{3}} \frac{\rho^{-n}\psi(\tau)^k}{n^{2/3}} \left(1 + O(n^{-1/3}(\log n)^4)\right). \tag{34}$$

By the the asymptotic forms (23), (26) of M_n, C_k, the last estimate renormalizes to give the probability of core size at $k = \alpha_0 n$:

(35)

$$\Pr(X_n = k) = \frac{C_k\, [z^n] H^k(z)}{M_n} = \frac{c_{3/2}}{m_{3/2}} \frac{g_1}{\kappa_3^{2/3}} \frac{\Gamma(2/3)}{2\pi\sqrt{3}} n^{-2/3} \left(1 + O(n^{-1/3}(\log n)^4)\right).$$

For nonseparable cores of general maps, one has $e^{K(z)} = (1+z)^2 (z(z-3)^2)^{1/3}/z$, $\tau = 1$, $\kappa_3 = 1/6$ and $g_1 = 3/2$ and the theorem follows as a specialization of Equation (35). □

A similar reasoning proves that the estimate remains valid for $n = 3k + e$ with e constant, and more generally for any e that does not grow "too fast" (in fact, $e = o(n^{2/3})$). It is interesting to contrast our approach with that of [7]: there, the authors use a circle centred at the origin that passes though the double saddle point; in other words, because the saddle point is double, the contour adopted in [7] is a stationary phase contour that does not benefit of strong concentration properties; accordingly the proof in [7] needs to appeal to estimates of oscillating integrals based on the method of Van der Corput, but the situation seems less favourable for deriving good error bounds. As we see next, our approach extends rather easily to a complete analysis in the central region.

2.3. **Nearby saddles.** When k is close to $\alpha_0 n$, we choose in the representation (29) an integration contour Γ that catches *simultaneously* the contributions of the two saddle points τ' and τ. For this purpose, we adopt a contour that goes through the mid-point, $\zeta := (\tau' + \tau)/2$, and, like in the previous case, meets the positive real line at an angle of $\pm 2\pi/3$. Local estimates of the integrand, once suitably normalized, lead to a complex integral representation that eventually reduces to Airy functions.

Theorem 3 (Local limit law and nearby saddles)**.** *The probability distribution of core-size admits a local limit law of the Airy type in the following sense: for any real numbers a, b, one has, as $n \to \infty$,*

$$\eta_n := \sup_{a \le \frac{k-\alpha_0 n}{n^{2/3}} \le b} \left| n^{2/3} \Pr(X_n = k) - p_\ell \, c\mathcal{A}\left(c \frac{k - \alpha_0 n}{n^{2/3}} \right) \right| \to 0, \tag{36}$$

with $p_\ell = \frac{1}{3}$ and $c = \frac{3}{4} 2^{2/3}$.

Proof. The proof parallels closely the one of Theorem 2. We set $k = \alpha_0 n + x n^{2/3}$ where x lies in a finite interval of the real line. The kernel is now a *perturbation* of the previous one: $K(z) = \log\left((\phi/z)\, \psi^{\alpha_0}\, \psi^{x n^{-1/3}} \right)$.

The contour of integration now comprises two small segments $\Delta_1^\circ, \Delta_2^\circ$ of length δ° meeting in $\zeta = (\tau' + \tau)/2$ at an angle $\pm 2\pi/3$ with the positive axis, completed by the arc of a circle simply encircling the origin. The quantity δ° is chosen like before and, for asymptotic purposes, we need only consider subparts Δ_1, Δ_2 of $\Delta_1^\circ, \Delta_2^\circ$ that have length $\delta = (\log n)\, n^{-1/3}$ satisfying (33) above.

We estimate the contribution $I_{1,2}$ arising from $\Delta_1 \cup \Delta_2$, which is the significant part of the contour. The distance between the two saddle points τ, τ' is $O(n^{-1/3})$ which represents the geometric "scale" of the problem. One thus sets $z = \zeta + u$ (with $|u| < n^{-1/3} \log n$). In the neighbourhood of ζ, local expansions of K and G are somewhat more complicated and are then best checked (with suitable monitoring) by a computer algebra system like `Maple`. The computation relies on the assumption $x = O(1)$, but some care in performing expansions is required because of the relations (33), namely $n\delta^3 \to \infty$ and $n\delta^4 \to 0$.

The local expansions of the functions $G(\zeta + u)$ and $K(\zeta + u)$ for x bounded and small u are found to be

$$\begin{aligned} K(\zeta + u) &= \kappa_0 - \kappa_0' x n^{-1/3} - \kappa_0'' x^3 n^{-1} + \kappa_1 x^2 u n^{-2/3} - \kappa_3 u^3 + O(n^{-4/3} \log^4 n), \\ G(\zeta + u) &= g_0 x n^{-1/3} - g_1 u + O(n^{-2/3} \log^2 n). \end{aligned}$$

There $\kappa_0, \kappa_0', \kappa_0'', \kappa_1, \kappa_3, g_0, g_1$ are computable positive numbers and the error terms are valid for $u \in \Delta_1 \cup \Delta_2$. The change of variable $u = vn^{-1/3}$ gives

$$\begin{aligned} I_{1,2} &= n^{-1/3} \int \left((g_0 x - g_1 v) n^{-1/3} + \epsilon_1 \right) e^{\kappa_0 n - \kappa_0' x n^{2/3} - \kappa_0'' x^3 + \kappa_1 x^2 v - \kappa_3 v^3 + \epsilon_2}\, dv \\ &= \exp(\kappa_0)^n\, n^{-2/3} \int \left((g_0 x - g_1 v) + n^{1/3} \epsilon_1 \right) e^{-\kappa_0'' x^3 + \kappa_1 x^2 v - \kappa_3 v^3} e^{\epsilon_2}\, dv \\ &= \exp(\kappa_0)^n\, n^{-2/3} \int (g_0 x - g_1 v) e^{-\kappa_0'' x^3 + \kappa_1 x^2 v - \kappa_3 v^3}\, dv\ (1 + O(\epsilon_2)). \end{aligned}$$

By convention, the variables ϵ_1 and ϵ_2 generically denote error terms that satisfy $\epsilon_1 = O\left(n^{-2/3}(\log n)^2\right)$ and $\epsilon_2 = O\left(n^{-1/3}(\log n)^4\right)$, and are uniform in x and n; integration takes place over the union of two segments Δ_1', Δ_2' each of length $\delta n^{1/3} = \log n$. Perform finally the change of variable $v = bt$ (with $b = (3\kappa_3)^{-1/3}$) and complete (introducing a negligible error) the integration path to $e^{\pm 2i\pi/3}\infty$:

$$\begin{aligned} [z^n] H(z)^k &= \frac{\exp(\kappa_0)^n}{2i\pi n^{2/3}} b^2 g_1 \int_{\infty e^{-2i\pi/3}}^{\infty e^{2i\pi/3}} \left(\frac{g_0}{w g_1} x - t\right) e^{-\kappa_0'' x^3 + \kappa_1 x^2 b t - \frac{t^3}{3}}\, dt\ (1 + \epsilon_2) \\ &= \exp(\kappa_0)^n\, n^{-2/3} c \mathcal{A}(cx)(1 + \epsilon_2). \end{aligned}$$

The reduction to $\mathrm{Ai}(x)$ and $\mathrm{Ai}'(x)$ is achieved by an integral representation equivalent to Definition 1 (see Appendix B for details). The Airy density function $\mathcal{A}$ involves the scaling factor $c = b g_1$ (also: $\kappa_0'' = \frac{2}{3} c^3$, $\kappa_1 b = c^2$, $\frac{g_0}{b g_1} = c$). In summary, for $x = O(1)$ and $k = \alpha_0 n + x n^{2/3}$, the main estimate found is

$$[z^n] H^k(z) = \frac{k}{n} \rho^{-n}\, \psi(\tau)^k\, n^{-2/3} c \mathcal{A}(cx) \left(1 + O(n^{-1/3}(\log n)^4)\right), \tag{37}$$

which gives eventually

$$\Pr(X_n = k) = n^{-2/3} p_\ell\, c \mathcal{A}(cx) \left(1 + O(n^{-1/3}(\log n)^4)\right) \tag{38}$$

For nonseparable cores of general maps, one finds $p_\ell = \frac{1}{3}$, $c = \frac{3}{4} 2^{2/3}$, and the statement follows. □

Theorem 3 together with the companion Theorem 7 below answer precisely a conjecture of Bender *et al.* in [7, p. 274], where the authors say (notations adjusted): *"we believe that for $|k - \alpha_0 n| = x n^{2/3}$ the probability is asymptotic to [some function] $\beta(x) n^{-2/3}$."*

The quantity η_n in (36) measures the "speed of convergence" of the discrete distributions of X_n to the Airy density limit. This speed is dictated by the error term ϵ_2 above, so that one has

$$\eta_n = O\left(n^{-1/3}(\log n)^4\right).$$

This error term can be improved to $O(n^{-1/3})$ provided expansions are pushed to the next order, and a complete asymptotic expansion could even be derived. We do not continue in this direction but turn instead to the analysis of coalescent saddle points that gives access to a wide region of k values—this however at the expense of a somewhat increased technical complexity.

Remark. The situation encountered with maps resorts to a general discussion of coefficients of the form

$$[z^n]\, \psi(z)^k \phi(z)^n$$

(with the possible addition of cofactors), this in critical regions where the basic saddle point method breaks down. The case of maps leads to coalescence between a fixed saddle point and a movable one, but other situations could be similarly dealt with[4]. Equivalently, the problem can be rephrased as one of estimating coefficients of trivariate rational functions,

$$[u^m v^k z^n] \frac{1}{(1-u\phi(z))(1-v\psi(z))}.$$

Under suitable conditions, an Airy phenomenon must take place when $m \approx n$ and $k \approx \alpha_0 n$. Pemantle [36] has launched an ambitious research programme that aims at relating asymptotic coefficient estimates to geometric properties of singular varieties and it would be of obvious interest to relate the present study to Pemantle's results. At least, our results indicate that Airy phenomena and, more generally, stable laws of rational index must be present in certain critical problems of multivariate asymptotic analysis.

3. Coalescing saddles

In the present section, we provide a uniform description of the transition regions around $n/3$, allowing k to vary in a wide region between $o(n)$ and $n-o(n)$. To this purpose, we set

$$k = \alpha_0 n + \beta n = (1/3+\beta)n,$$

with estimates valid uniformly for β in any compact subinterval of $]-\frac{1}{3},\frac{2}{3}[$.

Theorem 4 (Wide region and coalescent saddles)**.** *Let $k=(1/3+\beta)n$ for β in any compact subinterval of $]-\frac{1}{3},\frac{2}{3}[$. Then,* $\Pr(X_n = \lfloor n/3+\beta n\rfloor)$ *equals*

(39)
$$\frac{1}{3(1+3\beta)^{3/2}n^{2/3}}\left(\frac{a_1}{2}\mathcal{A}(n^{1/3}\xi)+\frac{a_4}{n^{2/3}}\exp\left(-\frac{2}{3}n\xi^3\right)\mathrm{Ai}(n^{2/3}\xi^2)\right)(1+O\left(1/n\right)),$$

where the quantities ξ, a_1, and a_4 depend only on β (we set $\mathrm{L}(x)=x\log x$):

$$\xi = \left(\frac{3}{2}\mathrm{L}(1+3\beta/2)+\frac{1}{2}\mathrm{L}(1-3\beta/2)-\frac{1}{2}\mathrm{L}(1+3\beta)\right)^{1/3}, \tag{40}$$

$$\frac{a_1}{2} = \frac{3}{4}\left(\frac{3\beta/\xi}{(1-9\beta^2/4)(1+3\beta)}\right)^{1/2} \quad \textit{and} \quad a_4 = \frac{2}{9\beta^2}\sqrt{\frac{3\xi}{\beta}}-\frac{a_1}{4\xi^2}. \tag{41}$$

The error term of (39) is uniform for β in any compact subinterval of $]-\frac{1}{3},\frac{2}{3}[$.

The estimates involve Airy functions composed with the quantity $n^{1/3}\xi$ that depends nonlinearly on β. In particular, Formula (39) extends the estimates of Section 2.3 when $k=n/3+xn^{2/3}$, since in that case $\beta\to 0$ while $n^{1/3}\xi$ is proportional to x, and the following approximations apply as $\beta\to 0$:

$$\frac{a_1}{2}=\frac{3}{4}2^{2/3}(1-5\beta/4)+O(\beta),\ a_4=-\frac{3}{8}2^{1/3}+O(\beta),\ \xi=\frac{3}{4}2^{2/3}(\beta-\beta^2/2)+O(\beta^3).$$

[4]Regarding the estimate at the centre, if at τ the cofactor G has a zero of order p and the kernel K has a saddle point of multiplicity q, then a factor $\Gamma(\frac{p+1}{q+1})$ should replace $\Gamma(\frac{2}{3})$. More generally, functions akin to stable laws (defined in Appendix A) of rational index are expected in the central region. We are however not aware at the moment of any natural combinatorial example involving saddle points of multiplicity larger than 2.

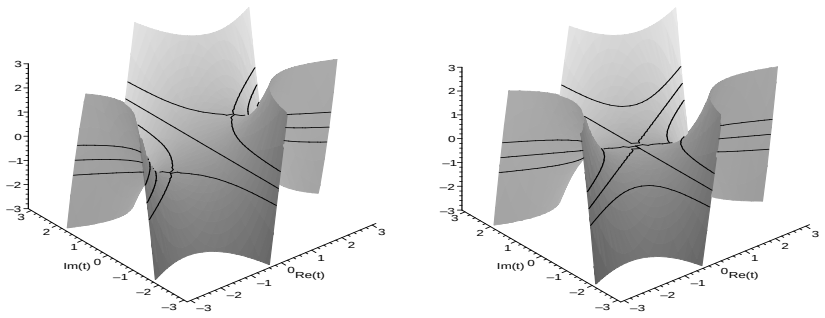

FIGURE 6. The landscape of $\Re(f(t))$ for $\xi = 1$ and $\xi = 0$.

This results in the following second order approximation, which is uniform in the central region $x = O(1)$ and refines Theorem 3: with $c = \frac{3}{4}2^{2/3}$,

$$\Pr(X_n = \lfloor n/3 + xn^{2/3} \rfloor) = \frac{c\mathcal{A}(cx)}{3n^{2/3}} \cdot \Big(1 - \big(\tfrac{13}{4} - \tfrac{cx}{2}\tfrac{\mathcal{A}'(cx)}{\mathcal{A}(cx)}\big)\, x\, n^{-1/3} + O(n^{-2/3})\Big)\,. \tag{42}$$

As soon as k leaves the $n/3 \pm O(n^{2/3})$ region, the two Airy terms in (39) start interfering and large deviations are then precisely quantified by (39). When k drifts away to the left of $n/3$ (and $n^{1/3}\xi \to -\infty$), basic asymptotics of Airy functions show that the formula simplifies to agree with the results of Section 2.1.

Proof. The transition phenomenon to be described is the coalescence of two simple saddle points into a double one. We follow the book of Bleistein and Handelsman [8, Sec. 9.2], where the method originally due to Chester, Friedman, and Ursell is exposed (see also [47]). The simplest occurrence of the phenomenon appears in the integration of $\exp(nf(t))$ with a cubic function f,

$$f(t) = \frac{t^3}{3} - \xi^2 t + r.$$

Indeed, in this case there are two saddle points $+\xi$ and $-\xi$ (given by $f'(t) = t^2 - \xi^2$), coalescing into a double saddle point as $\xi \to 0$. The landscape of $\Re(f(t))$ is represented on Figure 6 for $\xi = 1$ and $\xi = 0$. As expected, this landscape around $t = 0$ is very similar to the ones of Figure 4 near $z = 1$. The strategy consists in performing a change of variable in order to reduce the original problem (29) to this purely cubic case. Denote the kernel of the integral as $K(z) = \log(\psi^{k/n}\phi/z)$, with $k = (1/3 + \beta)n$ and the dependency on β kept implicit. The integral in (29) is

$$I(n, \beta) \quad = \quad \int_\Gamma G(z) \exp(nK(z)) dz,$$

where Γ is any contour that simply encircles the origin. In accordance with the discussion above, we seek a change of variable of the form

$$K(z) = -\left(t^3/3 - \xi^2 t\right) + r. \tag{43}$$

The parameters $\xi = \xi(\beta)$ and $r = r(\beta)$ must be chosen in order to map one landscape onto the other and in particular τ and τ' onto $+\xi$ and $-\xi$ respectively.

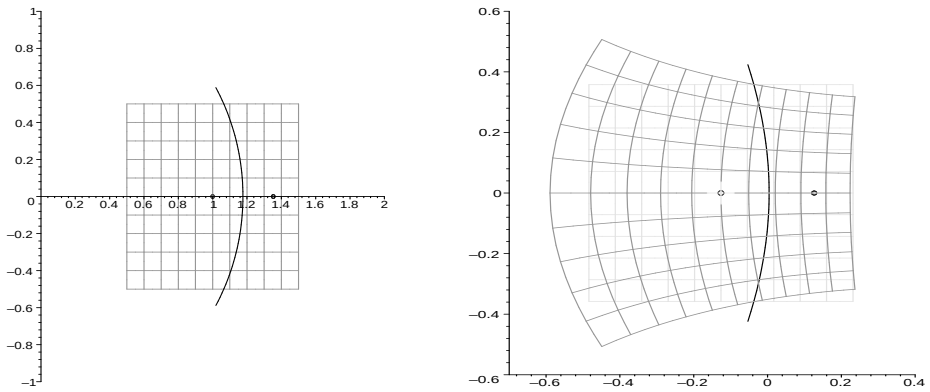

FIGURE 7. The conformal mapping $z \to t$ for $\beta = -1/10$: (i) A grid in the z-plane and a part of the path Γ; (ii) the corresponding images in the t-space.

This leads to the conditions

$$\begin{aligned} r &= \frac{1}{2}[K(\tau) + K(\tau')] = K(\tau) - \frac{2}{3}\xi^3 = \log(\psi(\tau)^{k/n}/\rho) - \frac{2}{3}\xi^3 \\ \xi^3 &= \frac{3}{4}[K(\tau) - K(\tau')]. \end{aligned} \tag{44}$$

There are three possibilities for ξ and we choose the real cubic root. In view of the values of K, ϕ and ψ, this leads to the definition (40).

The change of variable must satisfy (43) and map τ and τ' onto ξ and $-\xi$ respectively. In fact there exists a unique mapping $z \to t$ of this type that is conformal and sends the disc D of diameter $[\frac{1}{2}, \frac{3}{2}]$ to a domain D_β. Moreover, for β in $[-\frac{1}{10}, \frac{1}{10}]$, the image D_β contains the disc D' of diameter $[-\frac{1}{4}, \frac{1}{4}]$. In other words, it is possible to choose consistently for each z in D, an image t among the three branches allowed by (43). As illustrated by Figure 7, this mapping is very close to the linear mapping that sends τ and τ' onto ξ and $-\xi$.

The existence of this conformal mapping is proven in Appendix C. Let $z(t)$ be the inverse mapping and $G_0(t) = G(z(t))\dot{z}(t)$ where $\dot{z}(t) = \frac{dz}{dt}$. Remark that $G_0(t)$ is analytic in D', since the change of variable is conformal and $G(z)$ is analytic in D.

Next, we make the contour Γ precise and simultaneouly proceed with the estimation the integral. As is usual with saddle point integrals, we first need to localise the integral in D, neglecting the parts of the path down in valleys,

$$I(n, \beta) = \int_\Gamma G(z) \exp(nK(z))\, dz = \int_{\Gamma \cap D} G(z) \exp(nK(z))\, dz + \epsilon_1.$$

The geometry of the landscape immediately implies that the portion $\Gamma \setminus D$ of Γ can be chosen so as to wind about the origin while lying entirely in valleys, and we fix such choice once and for all. Consequently, the integral on $\Gamma \setminus D$ is bounded by the values at its endpoints, themselves fixed to be at $z = \tau_d + e^{\pm 2i\pi/3}$, with τ_d the dominant saddle point (the one closest to the origin). The error term then satisfies $\epsilon_1 = O(c^n) I(n, \beta)$ for some $0 < c < 1$, *i.e.*, it is exponentially negligible.

Inside the disc D we apply the change of variable (43), then restrict attention to the disc D', and deform the contour $\gamma \cap D$ into the relevant finite part of $\Delta_\infty = \{te^{\pm \frac{2i\pi}{3}},\, t \geq 0\}$:

$$\begin{aligned} I(n,\beta) &= \int_{\Gamma_\beta \cap D_\beta} G(z(t)) \exp(nf(t)) \dot{z}(t)\, dt + \epsilon_1 \\ &= \int_{\Delta_\infty \cap D'} G_0(t) \exp(nf(t))\, dt + \epsilon_2. \end{aligned}$$

As each end point is moved between two locations low in the valleys, the second error term ϵ_2 is again exponentially negligible.

In order to evaluate the last integral one needs to dispose of the cofactor $G_0(t)$. This is done via an integration by part. Since $G_0(\xi) = 0$ and G_0 is regular, taking $a_1 = G_0(-\xi)/(2\xi)$ leads to

$$G_0(t) = (\xi - t)a_1 + (t^2 - \xi^2)H_0(t),$$

where $H_0(t)$ is regular in D'. The expression (41) for a_1 follows from this definition using the value of $\dot{z}(-\xi)$ as computed in Appendix C. The integral $I(n,\beta)$ is then

$$I(n,\beta) = \exp(nr) \int_{\Delta_\infty \cap D'} (\xi - t) a_1 \exp\left(-n\left(t^3/3 - \xi^2 t\right)\right)\, dt + R_0,$$

where after integration by part, and up to another exponentially negligible term,

$$R_0 = \frac{\exp(nr)}{n} \int_{\Delta_\infty \cap D'} H_0'(t) \exp\left(-n\left(t^3/3 - \xi^2 t\right)\right)\, dt + \epsilon_3.$$

The integration by part has reduced the order of magnitude by a factor n, but because of the cancellation $G_0(\xi) = 0$, this second order term might interfere. Fortunately, R_0 is amenable to the same treatment as $I(n,\beta)$. Iterating the integration by part could lead to a complete expansion of $I(n,\beta)$ but we shall content ourselves with the next term, in which no further cancellation occurs. Set $H_0'(t) = a_2\xi + a_3 t + (t^2 - \xi^2)H_1(t)$, with $H_1(t)$ regular in D', and a_2, a_3 functions of β; we have

$$I(n,\beta) = \exp(nr) \int_{\Delta_\infty} \left(\xi\left(a_1 + \frac{a_2}{n}\right) - t\left(a_1 - \frac{a_3}{n}\right)\right) \exp\left(-n\left(t^3/3 - \xi^2 t\right)\right) dt + R_1.$$

where the integral has been extended to the whole of Δ_∞ at the expense of yet another exponentially negligible term. The error term is

$$R_1 = \frac{\exp(nr)}{n^2} \int_{\Delta_\infty \cap D'} H_1'(t) \exp\left(-n\left(t^3/3 - \xi^2 t\right)\right) dt + \epsilon_4.$$

In terms of the Airy function, we thus have directly

$$I(n,\beta) = 2i\pi \frac{\exp(nr)}{n^{2/3}} \left(\xi n^{1/3}\left(a_1 + \frac{a_2}{n}\right) \mathrm{Ai}(n^{2/3}\xi^2) - \left(a_1 - \frac{a_3}{n}\right) \mathrm{Ai}'(n^{2/3}\xi^2)\right) + R_1,$$

and the error term R_1 can be estimated: following [8, p. 375], there exist d_0 and d_1 positive such that

$$|R_1| \leq \frac{\exp(nr)}{n^2} \left(\frac{d_0}{n^{1/3}} |\mathrm{Ai}(n^{2/3}\xi^2)| + \frac{d_1}{n^{2/3}} |\mathrm{Ai}'(n^{2/3}\xi^2)|\right).$$

The theorem follows from formulae (29), (23), (26), (44) and the definition of the map–Airy law, upon setting $a_4 = (a_2 + a_3)\xi$. □

4. Singularity Analysis of the Composition Schema

There are two aspects to the enumeration of maps. One aspect relies on what we have called the "Lagrangean framework", and has been treated accordingly by suitable adaptations of the saddle point method. The other one employed by Gao and Wormald in [24] is further developed now: it exploits directly the fact that map generating functions like M, C, H each have a unique dominant singularity that is isolated and involves the singular exponent $\frac{3}{2}$. In this section, we provide an analysis of the probability law arising from *any* functional composition schema of singular exponent $3/2$ under the "criticality" assumption already encountered in Section 1.3; the abstract conditions are (45), (48), and (49) below. (Other non-critical cases turn out to be in fact simpler and are already known from [4, 23, 41] and related works.) We establish that the "map–Airy" distribution is due to appear systematically in such contexts. Technically, this section bases itself on the principles of Flajolet and Odlyzko's singularity analysis method [20, 35] and constitutes an alternative to the method of coalescing saddles.

As we aim at analysing combinatorial generating functions, we restrict attention in what follows to functions with *nonnegative coefficients* at 0. First, a function F analytic at 0 with radius of convergence r_F is said to be *singular with exponent* $\frac{3}{2}$ if the following conditions hold:

(45)
$$\begin{cases} F(z) \text{ is analytic on } |z| = r_F,\ z \neq r_F; \\ F(z) \text{ is continuable in } \Delta := \{\, z \;\mid\; |z| < R_F,\ z \notin [r_F, R_F] \,\}; \\ F(z) = f_0 - f_1\,(1 - z/r_F) + f_{3/2}\,(1 - z/r_F)^{3/2} + O((1 - z/r_F)^2) \text{ as } z \to r_F \text{ in } \Delta. \end{cases}$$

There, $f_0, f_1, f_{3/2}$ are positive constants and R_F is some constant satisfying $R_F > r_F$. This fact, by virtue of singularity analysis, entails

$$[z^n]F(z) \sim \frac{3}{4}\frac{f_{3/2}}{\sqrt{\pi}}\cdot\frac{r_F^{-n}}{n^{5/2}} \tag{46}$$

Next, as seen in Section 1, the equations describing core size are of the composition type. Given generating functions with nonnegative coefficients, C and H, we consider in the abstract the functional *composition schema*

$$M(z, u) = C(uH(z))$$

and the associated family of probability distributions

$$\Pr(X_n = k) = \frac{C_k}{M_n}\,[z^n]H(z)^k, \qquad C_k := [z^k]C(z), \quad M_n := [z^n]M(z, 1). \tag{47}$$

Combinatorially, this corresponds to a composition $\mathcal{M} = \mathcal{C} \circ \mathcal{H}$ between classes of objects, where objects of type $\mathcal{H}$ are substituted freely at individual "atoms" (*e.g.*, nodes, edges, or faces) of elements of $\mathcal{C}$. The bivariate generating function is such that $[z^n u^k]M(z, u)$ gives the number of $\mathcal{M}$–objects of total size n whose $\mathcal{C}$–component (the "core") has size k and X_n is the corresponding random variable describing core-size in this general context. We then define the composition schema $C(uH(z))$ to be of *singular type* $(\frac{3}{2} \circ \frac{3}{2})$ by the condition

$$C(z), H(z) \text{ have singular exponent } \tfrac{3}{2} \text{ in the sense of (45).} \tag{48}$$

In addition, the composition schema is said to be *critical* if there is exact coincidence between the singular value of H and the singularity of C:

$$H(r_H) = r_C. \tag{49}$$

(Criticality is satisfied in all composition schemas of maps examined in this paper.)

Here come a few basic observations on the "physics" of the counting problem. We denote the radii of convergence of C and H by $r_C = \sigma$ and $r_H = \rho$, and impose the condition $H(\rho) = \sigma$ expressing criticality (49). The local expansions are assumed to conform to (45):

(50)
$$\begin{array}{lllllllll} H(z) & = & \sigma & - & h_1(1-z/\rho) & + & h_{3/2}(1-z/\rho)^{3/2} & + & O((1-z/\rho)^2) \\ C(z) & = & c_0 & - & c_1(1-z/\sigma) & + & c_{3/2}(1-z/\sigma)^{3/2} & + & O((1-z/\sigma)^2). \end{array}$$

First, straight singularity analysis (see (45)) provides the asymptotic counts

$$H_n \equiv [z^n]H(z) \sim \frac{3h_{3/2}}{4\sqrt{\pi n^5}}\rho^{-n}, \quad C_k \equiv [z^k]C(z) \sim \frac{3c_{3/2}}{4\sqrt{\pi k^5}}\sigma^{-k},$$
$$M_n \equiv [z^n]M(z,1) \sim \frac{3m_{3/2}}{4\sqrt{\pi n^5}}\rho^{-n}, \qquad \text{where} \quad m_{3/2} := c_1\, h_{3/2}/\sigma + c_{3/2}(h_1/\sigma)^{3/2}.$$

Also, from the definition (47) of the distribution of core size X_n and the fact that any $C(z)^k$ has itself a singular expansion of exponent $\frac{3}{2}$, there results that

$$\Pr(X_n = k) \sim \frac{h_{3/2}}{m_{3/2}} k\, \sigma^{k-1} C_k, \tag{51}$$

for any *fixed* k. Thus, for bounded values of k, the probability decays initially roughly like

$$\frac{3h_{3/2}\, c_{3/2}}{4m_{3/2}\, \sigma\sqrt{\pi}} k^{-3/2}, \tag{52}$$

(as proved below, this estimate as $k \to \infty$ remains in fact valid as long as $k = o(n)$) and the $O(1)$ region of k contributes a total mass of about

$$p_s := c_1 h_{3/2}/(\sigma m_{3/2}). \tag{53}$$

Finally, the expectation of core size in a random $\mathcal{M}$–structure of size n is found by similar means to satisfy

$$E(X_n) = \frac{1}{M_n}[z^n]\left(\frac{\partial}{\partial u}C(uH(z))\right)_{u=1} \sim \left(\frac{c_{3/2}}{m_{3/2}}(h_1/\sigma)^{1/2}\right)\cdot n. \tag{54}$$

What is unusual is that the mean of X_n is $O(n)$, while the distribution assigns a fraction of the probability mass near the origin.

Theorem 5 (Composition Schema $(3/2 \circ 3/2)$)**.** *Consider a critical combinatorial schema $\mathcal{M} := \mathcal{C} \circ \mathcal{H}$ of type $(\frac{3}{2} \circ \frac{3}{2})$, with parameters as specified in* (50)*. The distribution of core size of a random element in $\mathcal{M}$ with size n has three asymptotic regimes depending on the value of k/n in comparison to*

$$\alpha_0 := \sigma/h_1.$$

(*i*) *For $k = \alpha n$, with $0 < \alpha < \alpha_0$, the* left tail *is polynomially small:*

$$\Pr(X_n = k) \;\sim\; \frac{3h_{3/2}\, c_{3/2}}{4m_{3/2}\, \sigma\sqrt{\pi}}\,(1-\alpha/\alpha_0)^{-5/2}\, k^{-3/2}\,.$$

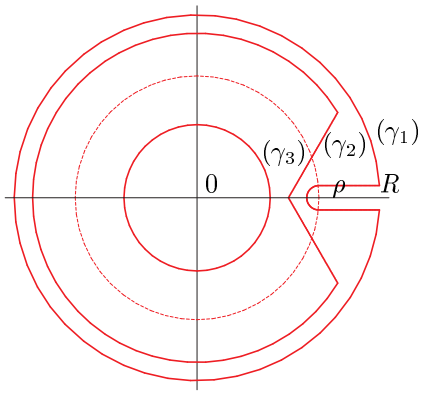

FIGURE 8. The three contours $(\gamma_1, \gamma_2, \gamma_3)$ corresponding to the three regimes of the distribution of core size (left tail, centre, right tail, resp.).

(*ii*) *In the* central region $k = \alpha_0 n + x n^{2/3}$ *with* $x = O(1)$, *an Airy law holds:*

$$n^{2/3} \Pr(X_n = \alpha_0 n + x n^{2/3}) \sim \alpha_0^{-3/2} \frac{c_{3/2}}{m_{3/2}} c\mathcal{A}(cx) \qquad \text{where } c = \frac{1}{\alpha_0} \left(\frac{h_1}{3 h_{3/2}} \right)^{2/3}.$$

(*iii*) *For* $k = \alpha n$, *with* $\alpha > \alpha_0$, *the* right tail *is exponentially small:*

$$\Pr(X_n = k) = O(A^k) \qquad \text{for some } A \equiv A(\alpha),\ 0 < A < 1.$$

Proof. The analysis[5] reduces to estimating coefficients of large powers of $H(z)$ and the starting point is Cauchy's coefficient formula

$$[z^n] H(z)^k = \frac{1}{2i\pi} \int_\gamma H(z)^k \frac{dz}{z^{n+1}} \tag{55}$$

now evaluated directly without reference to any parametrization. Contours corresponding to the three cases are depicted in Figure 8.

Common to cases (*i*) and (*ii*), we choose the contour γ as being composed of an arc of some circle of radius $R > \rho$ connected to a loop around $[\rho, R]$. The open loop approaches ρ at an angle $-\phi$ (where ϕ has to be strictly less than $\pi/2$) then winds around ρ while staying at a distance from ρ chosen to be n^{-r}, and then continues at an angle ϕ from the positive axis. (We shall take $\phi = 0$ and $r = 1$ for the left tail, $\phi = \pi/3$ and $r = 2/3$ for the central region.)

A technical point must be noted before we can proceed. Let D_R be the disk of radius R centred at 0. In what follows, we analyse large powers of $h(z) = H(z)^\alpha / z$ in parts of some D_R. Since $H(z)$ has nonnegative coefficients and a unique dominant singularity, along any circle centred at 0, it attains its maximum modulus uniquely on the positive real axis but this property does not necessarily hold *outside* of the disk of convergence $|z| = \rho$. However, if any fixed neighbourhood V of ρ is excluded, one can still ensure that $|H(z)| < H(\rho)$ and $|h(z)| < h(\rho)$ for $z \in D_R \setminus V$.

[5]To keep this section short, we only indicate the major analytic steps and do not attempt to make error terms systematically explicit or uniform (see however Figure 9 for indications). Details can be easily supplied by reference to the singularity analysis paper [20] as the approach is somewhat similar.

In the analysis described below, we also make use of local expansions near ρ and base the analysis on the fact that $|h(z)|$ decreases locally away from ρ along certain directions in a neighbourhood V of ρ. Again, this need not hold *globally*, but, by having restricted V suitably, we can always assume that this decrease holds throughout V. In what follows the contours γ that we choose are implicitly taken inside domains D_R, V that satisfy these requirements. In this way, we ensure two properties: (a) the contribution to (55) that is due to the arc of the larger circle is exponentially small compared to $\sigma^k \rho^{-n}$; (b) the dominant part of the integral arises from a vicinity of the singularity where local expansions are assumed to be globally valid. In particular, one has for z near ρ in a Δ-domain of the form (45):

(56)
$$h(z) \equiv \frac{H(z)^\alpha}{z} = \frac{\sigma^\alpha}{\rho}\left(1 + \left(1 - \frac{h_1\,\alpha}{\sigma}\right) Z + \frac{h_{3/2}\alpha}{\sigma} Z^{3/2} + O(Z^2)\right), \quad Z := 1 - \frac{z}{\rho}.$$

(The determinations are the principal ones when $Z > 0$, corresponding to z left of ρ.)

(i) *Left tail.* For this regime, the local expansion (56) shows that the function $h(z) = H(z)^\alpha / z$ decreases when going away from 1 parallel to the real axis since the coefficient of Z is positive when $\alpha < \alpha_0$ and Z has there a negative real part. The contour γ_1 adopted then includes a loop in the z–plane—this is exactly the Hankel contour of singularity analysis—passing at distance $1/n$ from the singularity and oriented positively. Only a small part of the contour, the "range", matters asymptotically. The standard change of variable $z = \rho(1 - t/n)$ is performed and, up to exponentially small terms, only the part $t \leqslant (\log n)^2$ of the contributes. Then the Cauchy kernel z^{-n} becomes, in the limit $n \to \infty$, the exponential kernel e^t multiplied by ρ^{-n}, and the expansion of $H(z)^k$ provides

$$\frac{H(z)^k}{z^{n+1}}\,dz = \frac{\sigma^k \rho^{-n}}{n} e^{\lambda t}\left(1 + \frac{k h_{3/2}}{\sigma}\frac{t^{3/2}}{n^{3/2}} + O(n^{-1.99})\right) dt, \quad \lambda := 1 - \frac{h_1}{\sigma}\frac{k}{n}. \tag{57}$$

In the t–plane, the image contour of γ_1 is now completed into a loop γ_1' coming from $-\infty - i$, encircling the origin on the right and going back to $-\infty + i$ (introducing again only exponentially small error terms). In the process, termwise integration of the expansion (57) against the kernel $e^{\lambda t}$ shows that the contribution of the term 1 is negligible (the complete integral $\int_{\gamma_1'} e^{\lambda t} dt$ is identically 0). One finds in this way that

$$\begin{aligned} [z^n] H(z)^k &\sim \frac{\sigma^k \rho^{-n}}{n^{5/2}} \frac{h_{3/2} k}{\sigma} \frac{1}{2i\pi} \int_{\gamma_1'} e^{t(1-\alpha h_1/\sigma)} t^{3/2}\, dt \\ &\sim \frac{\sigma^k \rho^{-n}}{\Gamma(-3/2) n^{5/2}} \frac{h_{3/2} k}{\sigma} (1 - \alpha h_1/\sigma)^{-5/2}, \end{aligned} \tag{58}$$

where the second line derives from Hankel's original representation of the Gamma function [46, Sec. 12.22]:

$$\frac{1}{\Gamma(s)} = \frac{1}{2i\pi} \int_{-\infty}^{(0+)} t^{-s} e^t\, dt.$$

From there, the left-tail estimates (i) result after normalization by

$$\frac{C_k}{M_n} \sim \frac{c_{3/2}}{m_{3/2}} \left(\frac{n}{k}\right)^{5/2} \sigma^{-k} \rho^n. \tag{59}$$

The formula (58) extends (52) provided k tends to infinity more slowly than $\alpha_0 n$, but it introduces a curious distortion factor of $(1-\alpha/\alpha_0)^{-5/2}$. The estimate obviously ceases to be valid when α approaches α_0.

(*ii*) *Central region.* In this case, we adopt as integration contour in the z–plane a contour γ_2 including a positively oriented "loop" that is made of two rays at an angle of $\pi/3$ and $-\pi/3$ with $(0,+\infty)$; also, the two rays intersect on the real axis left of the singularity, at a distance chosen to equal $\rho n^{-2/3}$.

When $\alpha = k/n$ is exactly at α_0, the term linear in Z disappears from (56). Also, the argument of $Z^{3/2}$ is $\pm\pi$ so that $h(z) = H(z)^\alpha/z$ decreases in modulus when going away from ρ. When k/n is within $O(n^{-1/3})$ from α_0, $|h(z)|$ decreases along the contour away from ρ provided Z is a bit larger than $n^{-2/3}$, say, $Z > n^{-2/3}\log^2 n$ (since, then, the terms involving $Z^{3/2}$ take over the terms linear in Z), and we may neglect the corresponding contribution to the integral as it is exponentially small (roughly like $\exp(-\log^3 n)$).

We perform the normalization $z = \rho(1 - t/n^{2/3})$ and, on the significant part of the contour, one has $t \leqslant \log^2 n$. First, an easy calculation shows that, in the range,

$$\frac{H(z)^k}{z^{n+1}}\,dz = -\frac{\sigma^k \rho^{-n}}{n^{2/3}} \exp\left(-\frac{h_1}{\sigma} x t + \frac{h_{3/2}}{h_1} t^{3/2} + O(n^{-0.33})\right) dt. \tag{60}$$

Next, the variable t evolves on a contour made of two segments of angle $2\pi/3$ and $-2\pi/3$, intersecting at -1, and each of length $O(\log^2 n)$. At the expense of exponentially small error terms, this contour can be extended back to infinity. Reverting the orientation and shifting the contour by 1, this results for t in the new contour composed of two infinite rays, and Equation (60) implies

$$[z^n]H(z)^k \quad\sim\quad \frac{\sigma^k \rho^{-n}}{n^{2/3}} \frac{1}{2i\pi} \int_{\infty e^{-2i\pi/3}}^{\infty e^{2i\pi/3}} \exp\left(\frac{h_{3/2}}{h_1} t^{3/2} - \frac{h_1}{\sigma} x t\right) dt\,.$$

The integral representation is one of the basic forms of the Airy distribution (see Appendix B). In summary, we have found a "central" estimate for large powers of H,

$$[z^n]H(z)^k \sim \frac{\sigma^k \rho^{-n}}{n^{2/3}} \frac{\sigma}{h_1}\, c\mathcal{A}(cx)$$

which, after the normalization (59), gives precisely the Airy density in the central region (*ii*). As a consistency check, note that the total mass concentrated near $\alpha_0 n$ comes out as $1 - p_s$, where p_s is the mass of the "small" k region (53); also the contribution to mean core-size due to the central region is $\sim \alpha_0(1-p_s)n$, which matches asymptotically the direct estimation in (54).

(*iii*) *Right tail.* Without loss of generality, we assume that $H(z)$ is of exact order z at 0 and consider accordingly $\alpha < 1$. Let ζ be any positive number strictly less than the radius of convergence ρ of $H(z)$. Since H has nonnegative coefficients, trivial bounds applied to coefficient integrals entail

$$[z^n]H(z)^k \leqslant \left(\frac{H(\zeta)^\alpha}{\zeta}\right)^n. \tag{61}$$

Let $h(z) = H(z)^\alpha/z$. One has trivially $h'(0^+) = -\infty$ while, at the other end, $h'(\rho) = \frac{\sigma^\alpha}{\rho^2}\left(\alpha\frac{h_1}{\sigma} - 1\right)$, a quantity that is strictly positive precisely when $\alpha > \sigma/h_1$. Thus $h(z)$ is decreasing away from 0 and increasing when z approaches ρ from the left. Consequently, it attains its minimum value at some point $\zeta_0 \in (0,\rho)$ and the

	Left tail	Central region	Right Tail
Method:	singularity analysis	this paper	saddle point
Type:	$\int e^t t^{3/2} dt \ \left(\Gamma(-\frac{3}{2})^{-1}\right)$	$\int e^{t^{3/2}-xt} dt \ \left(\mathrm{Ai}(x^2)\right)$	$\int e^{-t^2} dt \ \left(\Gamma(\frac{1}{2})\right)$
Angle (ϕ):	± 0	$\pm\frac{\pi}{3}$	$\pm\frac{\pi}{2}$
Dist. to sing.:	$\frac{1}{n}$	$\frac{1}{n^{2/3}}$	$O(1)$
Range:	$\frac{\log^2 n}{n}$	$\frac{\log^2 n}{n^{2/3}}$	$\frac{\log^2 n}{n^{1/2}}$
Error:	$n^{-1/2}$	$n^{-1/3+\epsilon}$	$n^{-1/2}$

FIGURE 9. Composition of singularities: The methods, types of normalized integrals, contours (angle, distance to singularity), effective ranges , and approximation errors corresponding to the three regimes of the law of core-size.

inequality $h(\zeta_0) < h(\rho) = \sigma^\alpha/\rho$ holds there. (In fact, the minimum is unique and thus determined by the relations: $h'(\zeta_0) = 0$ and $0 < \zeta_0 < \rho$.) Thus, from the bound (61) taken at $\zeta = \zeta_0$, one finds that $[z^n]H(z)^k \leqslant h(\zeta_0)^n$. Combining this last inequality with the known asymptotic forms of C_k and M_n shows that

$$\Pr(X_n = k) = O\left(\frac{h(\zeta_0)}{h(\rho)}\right)^n,$$

where ζ_0 is a computable function of α. This constitutes the exponentially small estimate of the right tail (*iii*), with $A = h(\zeta_0)/h(\rho)$. The point ζ_0 is in fact a saddle point of the integrand. As is true of coefficients of order n in powers of order n of "most" analytic functions (see *e.g.*, the survey [25]), the saddle point method applies. Here, it suffices to take as integration contour the circle of radius ζ_0 that is a saddle-point contour. In this way, the upper bound is easily refined into the asymptotic form $cA^n n^{-1/2}$. □

Closer inspection of the proof reveals that the error terms can be made uniform (see the last line of Figure 9): for the left tail, this requires α to be confined to a closed subinterval of $(0, \alpha_0)$ for the central region, uniformity is granted when x is restricted to any finite interval, which corresponds to $k = \alpha_0 n \pm O(n^{2/3})$.

It is quite striking to watch the interplay between the various regimes analysed and the choice of the corresponding contours. See Figure 9 for a summary, which is to be compared to Figure 5 for the saddle-point approach. As is expected from the general theory [20], when k remains $O(1)$, the usual Hankel contour (at distance $1/n$ from ρ) fully captures the singular behaviour of the generating functions (see (51)) and it continues to do so as long as k remains smaller than $\alpha_0 n$. As soon as the central region $k \approx \alpha_0 n$ is approached, the Hankel contour must be moved away from the singularity (at distance $n^{-2/3}$) while being folded back towards the circle of convergence. Finally, when k exceeds $\alpha_0 n$, the contour moves further back (it can be entirely folded within the disk of convergence) passing through a saddle point that is then at distance $O(1)$ from ρ.

5. Varieties of maps, largest components, and random sampling

The results obtained in the particular case of nonseparable cores of maps belong to a very general pattern in the physics of random maps. In this section, we first exhibit a dozen classes of maps that resort to the composition schema and the Lagrangean framework (Section 5.1). The analytic properties, in terms of either the associated saddle point geometry or the singularity structure, entirely parallel the treatment given for nonseparable core of general maps. Accordingly, an Airy law of the map type holds for multiconnected cores of several varieties of maps (Theorem 6). Next, in Section 5.2, we follow the lines of earlier works of Bender, Gao, Richmond, and Wormald and "transfer" the estimates of core-size to largest multiconnected components of random maps (Theorem 7). Various consequences for random sampling are given in Section 5.3, and we conclude with simulation results that validate well all our previous analyses (Section 5.4).

5.1. Map related composition schemas.

We start with a few definitions of classes of maps that have proved to be of interest in the combinatorial literature.

Families of maps. A map is *loopless* if it does not contain any loop; *bridgeless* if it does not contain any bridge (a bridge, or isthmus, is an edge whose removal disconnects the map); *simple* if it does not contain multiple edges nor loops; *bipartite* if the vertices can be coloured in two colours such that each edge is incident to both colours.

A map is *k-connected*, $k \geq 2$, if it cannot be separated into several connected components by removing $k-1$ vertices. A map is *nonseparable* if it is 2-connected and loopless, with an exception for the two maps with one edge (the bridge and the loop) that are taken to be nonseparable by convention.

A map is a *singular triangulation* if all its faces have degree three (including the outerface); it is a *triangulation* if moreover it is 3-connected (these correspond to the usual geometric triangulations, with straight line triangles and no multiple

Table 1. A selection of classical families together with their associated generating functions, $M(z) = \sum_{n\geq 1} M_n z^n$, where M_n is the number of maps in $\mathcal{M}$ that have size n.

maps, size $n \geq 1$	generating function (first terms)
$\mathcal{M}_1$ general maps, n edges	$M_1(z) = 2z + 9z^2 + 54z^3 + 378z^4 + 2916z^5$
$\mathcal{M}_2$ bridgeless maps, n edges	$M_2(z) = z + 3z^2 + 13z^3 + 68z^4 + 399z^5$
$\mathcal{M}_2$ loopless maps, n edges	$M_2(z) = z + 3z^2 + 13z^3 + 68z^4 + 399z^5$
$\mathcal{M}_3$ simple maps, n edges	$M_3(z) = z + 2z^2 + 6z^3 + 23z^4 + 103z^5$
$\mathcal{M}_4$ nonseparable maps, n edges	$M_4(z) = 2z + z^2 + 2z^3 + 6z^4 + 22z^5 + 91z^6$
$\mathcal{M}_5$ nonseparable simple maps, n edges	$M_5(z) = z + z^3 + z^4 + 6z^5 + 16z^6 + 71z^7$
$\mathcal{M}_6$ 3-connected maps, $n+1$ edges	$M_6(z) = z^5 + 4z^7 + 6z^8 + 24z^9 + 66z^{10}$
$\mathcal{B}_1$ bipartite maps, n edges	$B_1(z) = z + 3z^2 + 12z^3 + 56z^4 + 288z^5$
$\mathcal{B}_2$ bip. simple maps, n edges	$B_2(z) = z + 2z^2 + 5z^3 + 15z^4 + 52z^5$
$\mathcal{B}_3$ bib. bridgeless maps, n edges	$B_3(z) = z^2 + z^3 + 6z^4 + 16z^5 + 71z^6$
$\mathcal{B}_4$ bip. nonseparable maps, n edges	$B_4(z) = z + z^2 + z^3 + 2z^4 + 6z^5 + 19z^6$
$\mathcal{B}_5$ bip. nonsepar. simple maps, n edges	$B_5(z) = z + z^4 + 3z^6 + 7z^7 + 15z^8 + 63z^9$
$\mathcal{T}_1$ singular triangulations, $n+2$ vert.	$T_1(z) = z + 4z^2 + 24z^3 + 176z^4 + 1456z^5$
$\mathcal{T}_2$ triangulations, $n+3$ vert.	$T_2(z) = z + 3z^2 + 13z^3 + 68z^4 + 399z^5$
$\mathcal{T}_3$ irreducible triangulations, $n+3$ vert.	$T_3(z) = z + z^3 + 3z^4 + 12z^5 + 52z^6 + 241z^7$

edges); it is an *irreducible triangulation* if moreover all its cycles of length three bound a face. Observe that 3-connected maps are in one-to-one correspondence with *graphs of convex polyhedra*, and that irreducible triangulations are also called *4-connected maximal planar graphs*.

Table 1 illustrates these definitions by providing for various families the first few terms of their generating functions. We recall that the generating functions are for *rooted* maps. Historical references on the enumeration of these families can be found in [32].

Many families of maps have algebraic generating functions, that admit Lagrangean parametrizations of the form (4). Moreover, they normally have a unique dominant singularity and a singular exponent equal to $3/2$, with the validity of the singular expansion being as required by Theorem 5. Table 2 illustrates this "universal" phenomenon by providing the parametrizations, dominant singularity and singular expansion for the families of Table 1.

Composition schemas. Table 3 presents some interesting composition schemas relating the previous families. For each line of the table a basic family $\mathcal{M}$ and a core family $\mathcal{C}$ are given, together with four series $M(z)$, $C(z)$, $H(z)$ and $D(z)$. The series $M(z)$ and $C(z)$ are the generating function of the families $\mathcal{M}$ and $\mathcal{C}$ and are given in terms of the series of Table 2. Except for the last line, the composition schema has then the form

$$\mathcal{M} = \mathcal{C} \circ \mathcal{H} + \mathcal{D},$$

meaning that a map of $\mathcal{M}$ either has a core of $\mathcal{C}$ in which some substituands of $\mathcal{H}$ are attached, or has no core. In particular the bivariate generating function of maps with respect to the size of the core is then

$$M(z,u) = C(uH(z)) + D(z).$$

TABLE 2. Generating functions, parametrizations and singular expansions for the families of Table 1. In this table, $M(z) = \Psi(L(z))$, where $L(z) = z\phi(L(z))$.

$\mathcal{M}$	ϕ	Ψ	$1/\rho$	singular expansion ($Z = 1 - z/\rho$)
$\mathcal{M}_1$	$3(1+y)^2$	$\frac{2y-y^2}{3}$	12	$\frac{1}{3} - \frac{4}{3}Z + \frac{8}{3}Z^{3/2} + O(Z^2)$
$\mathcal{M}_2$	$3(1+\frac{y}{4})^4$	$\frac{y(y^2+3y-9)}{27}$	$\frac{256}{27}$	$\frac{5}{27} - \frac{16}{27}Z + \frac{32\sqrt{6}}{81}Z^{3/2} + O(Z^2)$
$\mathcal{M}_3$	$\frac{(y+3)^2}{3-y}$	$\frac{-y(y^2+3y-9)}{27}$	8	$\frac{5}{27} - \frac{32}{81}Z + \frac{256}{729}Z^{3/2} + O(Z^2)$
$\mathcal{M}_4$	$(1+y)^3$	$\frac{y(2+y-y^2)}{(1+y)^3}$	$\frac{27}{4}$	$\frac{1}{3} - \frac{4}{9}Z + \frac{8\sqrt{3}}{81}Z^{3/2} + O(Z^2)$
$\mathcal{M}_5$	$\frac{(y+1)^6}{(2y+1)^2}$	$\frac{y(-y^2+y+1)}{(y+1)^3}$	$\frac{729}{128}$	$\frac{5}{27} - \frac{32}{135}Z + \frac{2^8\sqrt{15}}{3^4 5^3}Z^{3/2} + O(Z^2)$
$\mathcal{M}_6$	$\frac{1}{1-y}$	$\frac{y^5(y^2+y-1)}{(1+y)^3(y^2-y-1)}$	4	$\frac{1}{540} - \frac{167}{8100}Z + \frac{32}{729}Z^{3/2} + O(Z^2)$
$\mathcal{B}_1$	$2(1+y)^2$	$\frac{y(2-y)}{4}$	8	$\frac{1}{4} - Z + 2Z^{3/2} + O(Z^2)$
$\mathcal{B}_2$	$\frac{8(1+y)^2}{4+2y-y^2}$	$\frac{y(2-y)}{4}$	$\frac{32}{5}$	$\frac{1}{4} - \frac{5}{9}Z + \frac{50\sqrt{5}}{243}Z^{3/2} + O(Z^2)$
$\mathcal{B}_3$	$\frac{(y+2)^6}{32(1+y)^2}$	$\frac{y^2(8-4y^2+4y-y^3)}{32(1+y)^2}$	$\frac{729}{128}$	$\frac{7}{128} - \frac{189}{640}Z + \frac{18\sqrt{15}}{125}Z^{3/2} + O(Z^2)$
$\mathcal{B}_4$	$\frac{32(1+y)^2}{(y^2-2y-4)^2}$	$\frac{y(2-y)}{4}$	$\frac{128}{25}$	$\frac{1}{4} - \frac{5}{13}Z + \frac{50}{2197}Z^{3/2} + O(Z^2)$
$\mathcal{B}_5$	$\frac{128(1+y)^2}{(4+2y-y^2)^3}$	$\frac{y(y-2)}{4}$	$\frac{512}{125}$	$\frac{1}{4} - \frac{5}{17}Z + \frac{50\sqrt{85}}{4931}Z^{3/2} + O(Z^2)$
$\mathcal{T}_1$	$2(1+y)^3$	$-\frac{y(y-1)}{2}$	$\frac{27}{2}$	$\frac{1}{8} - \frac{3}{8}Z + \frac{\sqrt{3}}{3}Z^{3/2} + O(Z^2)$
$\mathcal{T}_2$	$(1+y)^4$	$-y(y^2+y-1)$	$\frac{256}{27}$	$\frac{5}{27} - \frac{16}{27}Z + \frac{32\sqrt{6}}{81}Z^{3/2} + O(Z^2)$
$\mathcal{T}_3$	$\frac{1}{(y-1)^2}$	$\frac{y(y^2+y-1)}{(y-1)(1+y)^2}$	$\frac{27}{4}$	$\frac{5}{32} - \frac{27}{128}Z + \frac{9\sqrt{3}}{128}Z^{3/2} + O(Z^2)$

Let us now describe more specifically these schemas. Recall that maps are represented in the plane with the unbounded face on the right of the root; the *inside* of a cycle is then defined with respect to the unbounded face.

- The *loopless core of maps* is obtained by detaching all maximal loops and their interior (maximal means not contained within any other loop). Unless the root is a loop (this case gives $D(z)$), a loopless core is obtained. Conversely, at each of the $2k$ corners of a loopless map of size k, a sequence $(1/(1-\star))$ of loops with a map inside $(z(1+M))$ can be attached.
- The *bridgeless core of maps* is obtained by detaching all closest bridges (a bridge is closest if there are no other bridge between it and the root). Unless the root is a bridge a bridgeless core is obtained. Conversely, at each corner of a bridgeless map, a sequence of bridge leading to a submap can be attached. (This decomposition is dual to the previous one.)
- The *simple core of maps* is obtained by contracting all maximal cycles of length two into single edges. Conversely each edge of a simple core may be expanded into a cycle of length two containing a submap $((1+M))$.
- The *nonsingular core of singular triangulations* is just the *simple* core of singular triangulations so that the schema is essentially the previous one. The difference of $H(z)$ is only due to the different definition of size (size n means here $n+2$ vertices, thus $2n$ faces and $3n$ edges).
- The *nonseparable core of maps* was already discussed for general maps and works identically for bipartite maps.
- The *3-connected core of maps* is obtained cutting all maximal 2-separators and replacing the removed components by edges. This composition schema is described in [43].

The last schema, *irreducible core of triangulations*, is obtained by emptying all maximal 3-cycles and is described in [7]. It leads to a variant of the composition schema: the bivariate generating function is

$$M(z,u) = (1+M(z))C(uH(z)).$$

However this modification does not alter the applicability of our methods.

TABLE 3. Composition schemas, of the form $\mathcal{M} = \mathcal{C} \circ \mathcal{H} + \mathcal{D}$, except the last one where $\mathcal{M} = (1+\mathcal{M}) \times (\mathcal{C} \circ \mathcal{H})$.

maps, $M(z)$	cores, $C(z)$	submaps, $H(z)$	coreless, $D(z)$
all, $M_1(z)$	bridgeless, or loopless $M_2(z)$	$z/(1-z(1+M))^2$	$z(1+M)^2$
loopless $M_2(z)$	simple $M_3(z)$	$z(1+M)$	–
all, $M_1(z)$	nonsep., $M_4(z)$	$z(1+M)^2$	–
nonsep. $M_4(z)-z$	nonsep. simple $M_5(z)$	$z(1+M)$	–
nonsep. $M_4(z)/z-2$	3-connected $M_6(z)$	M	$z+2M^2/(1+M)$
bipartite, $B_1(z)$	bip. simple, $B_2(z)$	$z(1+M)$	–
bipartite, $B_1(z)$	bip. bridgeless, $B_3(z)$	$z/(1-z(1+M))^2$	$z(1+M)^2$
bipartite, $B_1(z)$	bip. nonsep., $B_4(z)$	$z(1+M)^2$	–
bip. nonsep., $B_4(z)$	bip. ns. smpl, $B_5(z)$	$z(1+M)$	–
singular tri., $T_1(z)$	triang., $z+zT_2(z)$	$z(1+M)^3$	–
triangulations, $T_2(z)$	irreducible tri., $T_3(z)$	$z(1+M)^2$	–

Core size. From the expansions of Table 2, it is mechanically verified that, for each schema $M = C(H) + D$, the dominant singularity of $C(z)$ is precisely $H(\rho)$, where ρ is the dominant singularity of both $M(z)$ and $H(z)$. Thus all the composition schemas listed are critical and the analysis of Section 4 applies directly. (The last schema involves a slight adaptation but clearly resorts to a similar analysis.) In addition, as shown by Table 2, all families of Table 1 obey the Lagrangean framework, Equation (4), and are thus amenable to the saddle point methods of Sections 2, 3 as well.

Theorem 6 (Airy law for varieties of maps)**.** *Consider any schema of Table 4 with parameters α_0, c and p_ℓ. The probability $\Pr(X_n = k)$ that a map of size n has a core of size k has a local limit law of the map–Airy type with centring constant α_0, scaling parameter c, and weight p_ℓ: uniformly for x in a bounded interval*

$$\Pr\left(X_n = \lfloor \alpha_0 n + x n^{2/3} \rfloor\right) = p_\ell \cdot \frac{c\mathcal{A}(cx)}{n^{2/3}} \left(1 + O(n^{-1/3})\right).$$

5.2. **The size of the largest component.** It was observed in [7, 24] that the size of the core is related to the size of the largest component in random maps. In order to make this assertion more precise, let us first consider again the case of nonseparable cores of maps.

The set of nonseparable components of a map is uniquely defined by the following procedure: as long as a component contains a separating vertex, cut this vertex into two. This decomposition does not depend on the order in which separating vertices are cut; in particular it can be obtained by extracting the core, as illustrated by Figure 2, and recursively applying the same decomposition to each submap. The core of a map is thus one of its components.

All schemas of Table 3 lead to similar notions of $\mathcal{C}$-components in $\mathcal{M}$-maps. The aim of this section is then to characterize the size X_n^* of the largest $\mathcal{C}$-components in random $\mathcal{M}$-maps of size n with uniform distribution.

Theorem 7 (Largest components and Airy law)**.** *Consider any schema of Table 4 with parameters α_0 and c. Let X_n^* be the size of the largest $\mathcal{C}$-component of in a random $\mathcal{M}$-map of size n with uniform distribution. Then*

$$\Pr\left(X_n^* = \lfloor \alpha_0 n + x n^{2/3} \rfloor\right) = \frac{c\mathcal{A}(cx)}{n^{2/3}} \left(1 + O(n^{-1/3})\right).$$

TABLE 4. Parameters of the composition schemas of Table 3.

maps	cores	α_0	c	p_ℓ
general, $\mathcal{M}_1$	bridge/loopless, $\mathcal{M}_2$	2/3	3/2	2/3
loopless, $\mathcal{M}_2$	simple, $\mathcal{M}_3$	2/3	$3^{4/3}/4$	2/3
general, $\mathcal{M}_1$	nonseparable, $\mathcal{M}_4$	1/3	$3/4^{2/3}$	1/3
nonsep., $\mathcal{M}_4$	nonsep. simple, $\mathcal{M}_5$	4/5	$15^{5/3}/36$	4/5
nonsep., $\mathcal{M}_4$	3-connected, $\mathcal{M}_6$	1/3	$3^{4/3}/4$	16/81
bipartite, $\mathcal{B}_1$	bip. simple, $\mathcal{B}_2$	5/9	$3^{8/3}/20$	5/9
bipartite, $\mathcal{B}_1$	bip. bridgeless, $\mathcal{B}_3$	3/5	$(15/2)^{5/3}/18$	3/5
bipartite, $\mathcal{B}_1$	bip. nonsep., $\mathcal{B}_4$	5/13	$(13/6)^{5/3} \cdot 3/10$	5/13
bip. nonsep., $\mathcal{B}_4$	bip. nonsep. simple, $\mathcal{B}_5$	5/17	$(17/3)^{5/3} \cdot 3/20$	5/17
singular tri., $\mathcal{T}_1$	triangulations, $\mathcal{T}_2$	1/2	$(3/2)^{1/3}$	1/2
triangulations, $\mathcal{T}_2$	irreducible tri., $\mathcal{T}_3$	1/2	$6^{2/3}/3$	729/2048

uniformly for x in any bounded interval.

Theorem 7 is proven in Appendix D. It extends precisely results of Bender *et al.* [7, 24] who proved that the largest component is with high probability concentrated near $\alpha_0 n$. To wit:

$$\Pr\left(|X_n^* - \alpha_0 n| < \lambda(n) n^{2/3}\right) \underset{n\to+\infty}{\longrightarrow} 1, \tag{62}$$

where $\lambda(n)$ is any function going to infinity with n. The following proposition completes Theorem 7, and immediately follows from [24, Lemma 4].

Proposition 5. *The second largest $\mathcal{C}$-component of a random $\mathcal{M}$-map of size n has almost surely size $O(n^{2/3})$.*

Theorem 7 and Proposition 5 provide an appealing interpretation of the bimodal behaviour of the core. Indeed, it can be rephrased as follows for nonseparable components of random maps: *A random map $\mathfrak{m}$ has almost surely a largest nonseparable component of size map-Airy distributed around $n/3$.*

Now choose a new root r for $\mathfrak{m}$ among its n edges. There are two possibilities: (i) with probability $1/3$, r belongs to the largest component and the core has size map-Airy distributed around $n/3$; (ii) with probability $2/3$, r misses the largest component and the core is a small component of size almost surely at most $O(n^{2/3})$. The two modes of the distribution X_n correspond precisely to these two cases.

Finally similar estimates involving the Airy distribution apply to unrooted maps:

Theorem 8 (Unrooted maps)**.** *The Airy law for largest components (Theorem 7) and the estimates of second largest components (Proposition 5) hold for random unrooted maps.*

The fact that unrooting does not affect asymptotic distributional properties usually holds true for a parameter of random maps whose definition does not depend on the root. Indeed the number of distinct rootings of an unrooted map with n edges is equal to $2n$ unless the map has a symmetry. But the probability that a random unrooted map has a symmetry is exponentially small in all families of Table 2, a fact that follows from the elegant analysis of Richmond and Wormald in [38]. The proof is then easily completed by following [38].

5.3. **Random sampling algorithms.** Random sampling algorithms for various families of maps have been described by Schaeffer in [39, 40]. Here, we show that all classes of maps described in Section 5.1 are amenable to efficient random generation and that the Airy distribution plays a rôle in the fine tuning of the corresponding algorithms.

First, there are four classes of maps which benefit of bijective equivalence with simpler combinatorial objects and, consequently, can be generated directly: general maps ($\mathcal{M}_1$), nonseparable maps ($\mathcal{M}_4$), bipartite maps ($\mathcal{B}_1$), and singular triangulations ($\mathcal{T}_1$). For these, one has available an algorithm, hereafter called `Map`, that relies on *conjugacy classes of trees*; see [39, 40] and also [10] for some new families. Given an integer n, `Map` outputs in linear time a map of size n, taken uniformly at random. For the purposes of the present article we take the algorithm `Map` (in its four variants) as granted.

Next, the algorithm, hereafter called `Core`, is a probabilistic algorithm based on the *extraction/rejection* method. This algorithm is described in Figure 10. For any composition schema (of the type $\mathcal{C}$-components in $\mathcal{M}$-maps), given an integer k, `Core` calls the algorithm `Map` as a black box and, by extracting cores till the

Probabilistic algorithm `Core(k)` with control function $f(k)$
repeat
1. Call `Map(n)` to generate a random map $\mathfrak{m} \in \mathcal{M}_n$ of size $n = f(k)$;
2. extract the core $\mathfrak{c}$ of $\mathfrak{m}$ with respect to the schema;
until $\mathfrak{c}$ has size k;
output $\mathfrak{c}$; $\{\mathfrak{c}$ is uniform in the core class $\mathcal{C}_k\}$.

FIGURE 10. The extraction/rejection algorithm `Core`.

"right" size k is encountered, it produces uniformly an element of $\mathcal{C}_k$. The `Core` algorithm applies directly to the classes of Tables 3 and 4 that appear as cores of $\mathcal{M}_1, \mathcal{M}_4, \mathcal{B}_1, \mathcal{T}_4$, namely, $\mathcal{M}_2, \mathcal{M}_5, \mathcal{M}_6, \mathcal{B}_2, \mathcal{B}_3, \mathcal{B}_4, \mathcal{T}_2$. The remaining classes, $\mathcal{M}_3, \mathcal{B}_5, \mathcal{T}_3$ are "cores of cores": for these, one observes that critical composition schemas are closed under composition (with the parameters α_0 and p_ℓ that are then to be composed multiplicatively), so that "cores of cores" are eventually amenable to the `Core` algorithm.

We now examine complexity issues related to the rejection principle of `Core`. The expected number of iterations ℓ_k made by `Core` satisfies the exact relation $\ell_k = \Pr(X_n = k)^{-1}$. The choice $f(k) = k/\alpha_0$ that was proposed in [40] yields for instance

$$\ell_k \sim \frac{1}{p_\ell c \mathcal{A}(0)} (k/\alpha_0)^{2/3}.$$

However, the cost gets improved if one maximizes $\Pr(X_n = k)$ for a given value k. In particular, it proves advantageous to make use of the peak of the Airy distribution.

We also note that a simple variation, `Largest`, of the algorithm `Core` consists in extracting at Step 2 the largest component instead of the core. The `Largest` algorithm is only almost-uniform (*i.e.*, uniform safe for a set of asymptotically negligible measure, corresponding to maps with nonunique largest components). In the analysis of the number of iterations, the probability $\Pr(X_n = k)$ has then to be replaced by $\Pr(X_n^* = k)$. We have:

Theorem 9 (Exact-size random sampling)**.** *For all core classes of Table 4, the choice $f(k) = k/\alpha_0$ yields a uniform random generator* `Core(k)` *whose average number of iterations satisfies*

$$\ell_k \sim \frac{1}{p_\ell c \mathcal{A}(0)} (k/\alpha_0)^{2/3}.$$

Let $x_0 \approx 0.44322$ be the position of the peak of the map-Airy density function ($(1 - 4x_0^3)\mathrm{Ai}(x_0^2) + 4x_0^2 \mathrm{Ai}'(x_0^2) = 0$). Then the optimal choice $\widehat{f}(k) = k/\alpha_0 - \frac{x_0}{\alpha_0 c}(k/\alpha_0)^{2/3}$ reduces further the expected number of iterations to

$$\widehat{\ell}_k \sim \frac{1}{p_\ell c \mathcal{A}(x_0)} (k/\alpha_0)^{2/3},$$

hence eliminating on average $1 - \mathcal{A}(0)/\mathcal{A}(x_0) \approx 30\%$ of iterations.

Similar results hold for the almost-uniform random generator `Largest`*, whose complexity is smaller by a factor $\sim p_\ell$.*

As explained in [39, 40], a call of the algorithm `Map` and the extraction of the core or of the largest component for the schemas of Table 3 take linear time. This proves that the extraction/rejection algorithms have overall complexity $O(k^{5/3})$.

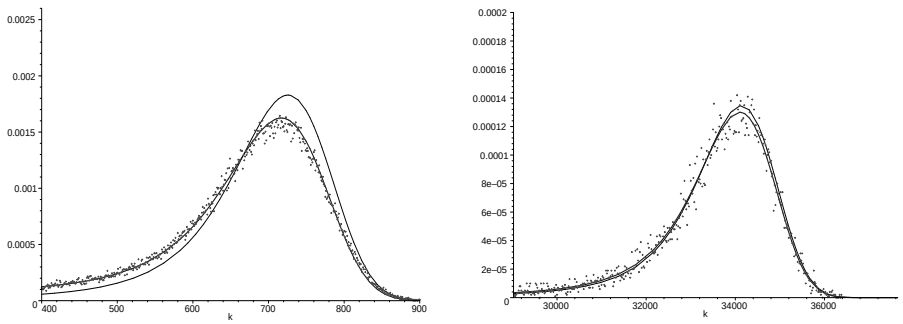

FIGURE 11. Core-size: Experimental results in the central region for $n = 2,000$ (left) and $n = 100,000$ (right), against first and second order approximations given by Theorems 6 and Formula (42).

The complexity can be further reduced by allowing some tolerance on the size of the map generated. In these variants, the algorithm is terminated as soon as a map of size $k \pm \Delta = [k - \Delta, k + \Delta]$ is obtained.

Theorem 10 (Approximate-size random sampling)**.** *The number of iterations of the algorithm* `Core`$(k \pm \Delta)$ *satisfies*

$$\ell_k(\Delta) = O\left(\frac{k^{2/3}}{\Delta}\right) + 1.$$

In particular, this algorithm, as well as its companion `Largest`$(k \pm \Delta)$*, becomes linear as soon as* $\Delta \geqslant \theta\, k^{2/3}$ *for some constant* θ*.*

Regarding unrooted maps, both `Map` and `Core` give rise to almost uniform random generators because the number of maps with a symmetry is exponentially small [38].

5.4. **Experimental results.** The random sampling algorithm `Map` has linear complexity and is thus very efficient: on a standard PC the generation speed is about 100,000 edges per second. Full decomposition in nonseparable components is linear as well and increases the cost of generation by a factor at most 2. This speed allows to produce very easily experimental observations of the results of the paper.

Figure 3 presents the observed frequencies of core-sizes for a sample of 50,000 maps with 2,000 edges. The theoretical curve as given by Theorem 4 fits perfectly the data on the full range $k \geq 10$, and upon using exact values for C_k, $k = 1 \ldots 9$, the fit is complete.

Figure 11 presents a region of width $n^{2/3}$ around $k = \alpha_0 n$ for two samples: 50,000 maps with 2,000 edges on the left hand side; 50,000 maps with 100,000 edges (with frequencies averaged over intervals of 20) on the right hand side. On each sample two theoretical curves are given, namely the local approximation of Theorem 6 and the second order approximation, Formula (42). While the second order curves fit perfectly the experimental data, the first order curve on the left hand side clearly displays an expected discrepancy of about $n^{-1/3} = 8\%$ for $n = 2,000$.

Figure 12 illustrates the result of Theorem 7: the size of the largest component in random maps. Again the sample has 50,000 maps with 2,000 edges and the fit with the theoretical curve is perfect, in a range much larger than expected (upon using again second order approximations). It is very interesting to note that the

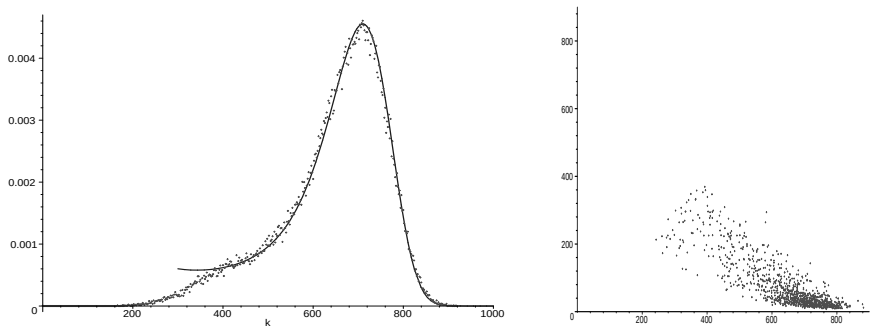

FIGURE 12. Left: Largest component sizes for $n = 2,000$, and predictions of Theorem 7. Right: Largest against second largest component sizes for 1,000 maps with 2,000 edges.

experimental curve presents a non regular point at $k \approx 400$ and starts decreasing much faster. This phenomenon probably occurs when the second largest component becomes almost as large as the first with high probability.

The interplay between the largest and second largest components is investigated more closely on the right hand side of Figure 12: the x-axis and y-axis correspond respectively to the sizes of the largest and second largest components and a sample of 1,000 maps of size 2,000 has been represented. Again it is worth pointing out that the value $k \approx 400$ corresponds to the largest size observed for which the second largest component has about the same size as the first.

6. Conclusion

The term of "universality" borrowed from statistical physics characterizes well the approach of our paper. By this is meant the isolation of phenomena that obey a common law whose global shape does not depend on specific details of the model. Here, we diagnose the existence of a "universality class" within analytic combinatorics, corresponding to coalescence of saddle points and confluence of singularities. A tangible sign is the occurrence of probability distributions and asymptotic estimates that involve the Airy function.

Despite the successes of the method of coalescing saddle points developed by applied mathematicians since the 1950's, we are only aware of scanty traces of the method being used in combinatorial enumerations. A special mention must however be made of Prellberg's paper [37] that provides an analysis of the area-perimeter generating function of staircase polygons in a "tri-critical region". (A technically difficult double inversion would still be required in order to transform Prellberg's estimates into enumerative or probabilistic results.) Roughly, two major orbits of problems seem to resort to a precise analysis of coalescence in saddle point landscapes.

(*i*) Large assemblies in critical regions must, under suitable singular conditions (Section 4, Appendix A), lead to an Airy law of the map type (and more generally to stable densities). There, the density is, as we saw, directly expressible in terms of the Airy function.

(*ii*) Brownian excursion area involves a different type of Airy law, of the "area type", of which the moments are generated by the logarithmic derivative

$\mathrm{Ai}'(z)/\mathrm{Ai}(z)$; see for instance [19] for an analytic discussion. As it is suggested by [37], it would be of great interest to develop a purely analytic connection between coalescing saddle points and the various combinatorial models that lead to the Airy law of the "area type". Candidates already mentioned in the introduction include displacement in parking allocations and hashing, path length in trees, as well as area under walks and polyominoes.

The Airy distribution of the area type also intervenes in the study of connectivity in random graphs and, from the recent work [22], it is at least known that an analytic approach based on coalescing saddle points can provide nontrivial quantitative estimates.

Appendix A. Powers, Compositions, and Stable Laws

This section builds upon the technology introduced in Section 4 and more specifically on the proof of Theorem 5. We will see here that a mild extension of the method gives access to the analysis of powers of generating functions with algebraic–logarithmic singularities. This models large assemblies of combinatorial objects. An immediate consequence is the analysis of the size of the "core" in a composition $\mathcal{C}\circ\mathcal{H}$ as soon as the associated generating functions are algebraic–logarithmic. What appears systematically in this context is a collection of functions closely related to stable laws that are well-known in probability theory to arise as limit distributions of sums of independent random variables.

In what follows, we consider a generating function $H(z)$ that has nonnegative coefficients and a unique isolated singularity at its radius of convergence ρ, so that it satisfies the first two conditions of Equation (45) (with $\rho = r_H$). We shall relax the third condition of Equation (45) and consider more generally functions with a singular exponent $\lambda \notin \mathbb{N}$, which corresponds to a dominant singular term of the form $(1 - z/\rho)^\lambda$ in the local singular expansion. The discussion is focussed on the three ranges of λ: $(0,1)$, $(1,2)$, and $(2,+\infty)$.

Theorem 11. *For any parameter $\lambda \in (0,2)$, define the entire function*

$$G(x,\lambda) := \begin{cases} \dfrac{1}{\pi}\displaystyle\sum_{k\geqslant 1}(-1)^{k-1}x^k\frac{\Gamma(1+\lambda k)}{\Gamma(1+k)}\sin(\pi k\lambda) & (0<\lambda<1) \\ \dfrac{1}{\pi x}\displaystyle\sum_{k\geqslant 1}(-1)^{k-1}x^k\frac{\Gamma(1+k/\lambda)}{\Gamma(1+k)}\sin(\pi k/\lambda) & (1<\lambda<2) \end{cases} \tag{63}$$

The coefficient of z^n in a large power $H(z)^k$ of a fixed algebraic–logarithmic function $H(z)$ with singular exponent λ admits the following asymptotic estimates.

(i) For $0<\lambda<1$, that is, $H(z) = \sigma - h_\lambda(1-z/\rho)^\lambda + O(1-z/\rho)$, and when $k = xn^\lambda$, with $x = O(1)$ in any compact subinterval of $(0,+\infty)$, there holds

$$[z^n]H^k(z) \;\sim\; \sigma^k\rho^{-n}\frac{1}{n}\,G\left(\frac{xh_\lambda}{\sigma},\lambda\right). \tag{64}$$

(ii) For $1<\lambda<2$, that is, $H(z) = \sigma - h_1(1-z/\rho) + h_\lambda(1-z/\rho)^\lambda + O((1-z/\rho)^2)$, when $k = \frac{\sigma}{h_1}n + xn^{1/\lambda}$, with $x = O(1)$ in any compact subinterval of $(-\infty,+\infty)$, there holds

$$[z^n]H^k(z) \;\sim\; \sigma^k\rho^{-n}\frac{1}{n^{1/\lambda}}(h_1/h_\lambda)^{1/\lambda}G\left(\frac{xh_1^{1+1/\lambda}}{\sigma h_\lambda^{1/\lambda}},\lambda\right). \tag{65}$$

(iii) For $\lambda > 2$, a Gaussian approximation holds. In particular, for $2 < \lambda < 3$, that is, $H(z) = \sigma - h_1(1 - z/\rho) + h_2(1 - z/\rho)^2 - h_\lambda(1 - z/\rho)^\lambda + O((1 - z/\rho)^3)$, when $k = \frac{\sigma}{h_1} n + x\sqrt{n}$, with $x = O(1)$ in any compact subinterval of $(-\infty, +\infty)$, there holds

$$[z^n]H^k(z) \sim \sigma^k \rho^{-n} \frac{1}{\sqrt{n}} \frac{\sigma/h_1}{a\sqrt{2}\pi} e^{-x^2/2a^2} \qquad \text{with } a = 2(\tfrac{h_2}{h_1} - \tfrac{h_1}{2\sigma})\sigma^2/h_1^2. \tag{66}$$

Proof. The proofs are similar to the proof of Theorem 5, Case *(ii)*, and just require a suitable adjustment of the geometry of the Hankel contour and of the corresponding scaling.

Case (i). A classical Hankel contour, with the change of variable $z = \rho(1 - t/n)$, yields the approximation

$$[z^n]H^k(z) \sim -\frac{\sigma^k \rho^{-n}}{2i\pi n} \int e^{t - \frac{h_\lambda x}{\sigma} t^\lambda}\, dt$$

The integral is then simply estimated by expanding $\exp(-\frac{h_\lambda x}{\sigma} t^\lambda)$ and integrating termwise

$$[z^n]H^k(z) \sim -\frac{\sigma^k \rho^{-n}}{n} \sum_{k \geqslant 1} \frac{(-x)^k}{k!} \left(\frac{h_\lambda}{\sigma}\right)^k \frac{1}{\Gamma(-\lambda k)}, \tag{67}$$

which is equivalent to Equation (64), by virtue of the complement formula for the Gamma function.

Case (ii). When $1 < \lambda < 2$, the contour of integration in the z-plane is chosen to be a positively oriented loop, made of two rays of angle $\pi/(2\lambda)$ and $-\pi/(2\lambda)$ that intersect on the real axis at a distance $1/n^{1/\lambda}$ left of the singularity. The coefficient integral of H^k is rescaled by setting $z = \rho(1 - t/n^{1/\lambda})$, and one has

$$[z^n]H^k(z) \sim -\frac{\sigma^k \rho^{-n}}{2i\pi n^{1/\lambda}} \int e^{\frac{h_\lambda}{h_1} t^\lambda} e^{-\frac{x h_1}{\sigma} t}\, dt.$$

There, the contour of integration in the t-plane comprises two rays of angle π/λ and $-\pi/\lambda$, intersecting at -1. Setting $u = t^\lambda h_\lambda / h_1$, the contour transforms into a classical Hankel contour, starting from $-\infty$ over the real axis, winding about the origin, and returning to $-\infty$. So, with $\alpha = 1/\lambda$, one has

$$[z^n]H^k(z) \sim -\frac{\sigma^k \rho^{-n}}{2i\pi n^\alpha}\, \alpha \left(\frac{h_1}{h_\lambda}\right)^\alpha \int e^u\, e^{-\frac{x h_1^{\alpha+1}}{\sigma h_\lambda^\alpha} u^\alpha}\, u^{\alpha-1}\, du.$$

Expanding the exponential, integrating termwise, and appealing to the complement formula for the Gamma function finally reduces this last form to (65).

Case (iii). When $2 < \lambda < 3$, the angle ϕ of the contour of integration in the z–plane is chosen to be $\pi/2$, and the scaling is $\sqrt{n}$: under the change of variable $z = \rho(1 - t/\sqrt{n})$, the contour is transformed into two rays of angle $\pi/2$ and $-\pi/2$ (*i.e.*, a vertical line), intersecting at -1, and

$$[z^n]H^k(z) \sim -\frac{\sigma^k \rho^{-n}}{2i\pi\sqrt{n}} \int e^{pt^2 - \frac{h_1 x}{\sigma} t}\, dt,$$

with $p = \frac{h_2}{h_1} - \frac{h_1}{2\sigma}$. Complementing the square, and letting $u = t - \frac{h_1 x}{2p\sigma}$, we get

$$[z^n]H^k(z) \sim -\frac{\sigma^k \rho^{-n}}{2i\pi\sqrt{n}} e^{-\frac{h_1^2}{4p\sigma^2} x^2} \int e^{pu^2}\, du,$$

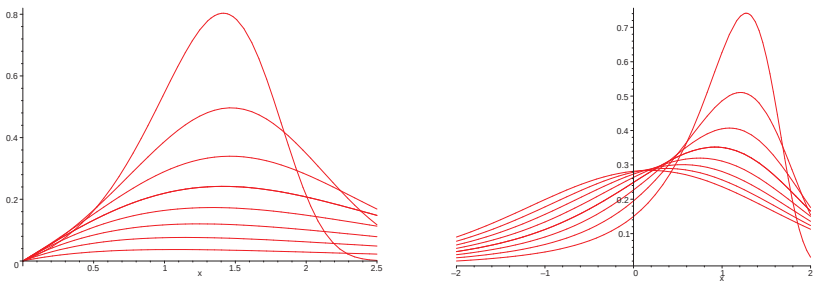

FIGURE 13. The G-functions for $\lambda = 0.1\,..\,0.8$ (left; from bottom to top) and for $\lambda = 1.2\,..\,1.9$ (right; from top to bottom); the thicker curves represent the Rayleigh law (left, $\lambda = \frac{1}{2}$) and the Airy law (right, $\lambda = \frac{3}{2}$).

which gives Equation (66). By similar means, such a Gaussian approximation can be shown to hold for any non-integral singular exponent $\lambda > 2$. □

We observe that the function G reduces to a (generalized) hypergeometric form when λ is rational. It is in all cases expressible in terms of the density of a *stable law*[6] of index $\min(\lambda, 2)$. (Note: the Gaussian law is a particular stable law of index 2.) A comparison between our methods and Feller's treatment also shows the striking similarity of computations in both cases.

We now list a few applications.

(*a*) *Local Limit theorems for sums of generalized Zipf laws.* The generalized Zipf law of parameter $s > 1$ is the law of a random variable Z defined by

$$\Pr(Z = k) = \frac{1}{\zeta(s)}\,\frac{1}{k^s},$$

where $\zeta(s)$ is the Riemann zeta function. It was proved in [17] that the probability generation function of Z satisfies precisely the conditions of singularity analysis (*i.e.*, it is continuable and admits a singular expansion valid outside of the unit circle) with the singular exponent being $\lambda = s - 1$. Hence, *the sum of a large number of independent copies of the Zipf law of parameter* $s \in (1, 3)$ *satisfies a* local *limit law of the stable type with parameter* $s - 1$. More generally, local limit laws of the stable variety will hold for sums of random variables whose probability generating function are algorithmic-logarithmic and continuable.

(*b*) The case $\lambda = 1/2$ covers many generating functions associated to combinatorial structures that are implicitly (or recursively) defined and have accordingly generating functions with a square-root singularity. This includes the varieties of simple trees introduced by Meir and Moon in [34]. Then, one has

$$G(x, \frac{1}{2}) = \frac{x}{2\sqrt{\pi}} \exp(-x^2/4), \quad [z^n]H^k(z) \;\sim\; \frac{\sigma^k \rho^{-n}}{n}\, G(x\frac{h_\lambda}{\sigma}, \frac{1}{2}).$$

[6] In probability theory, stable laws are defined as the possible limit laws of sums of independent identically distributed random variables. The function G above is a trivial variant of the density of the stable law of index λ; see Feller's book [16, p. 581–583]. Valuable informations regarding stable laws may be found in the books by Breiman [11, Sec. 9.8], Durett [15, Sec. 2.7], and Zolotarev [48].

The law with density proportional to $xe^{-x^2/4}$ is known as the Rayleigh law: it has been detected in simple trees by Meir and Moon who base their analysis on a Lagrangean change of variable and on the saddle point method. A consequence of [34] and of Theorem 11 is then: *The profile of a large tree in a simple family obeys a Rayleigh law in the asymptotic limit.* Similar results apply to $T(z)$, the Cayley tree function ($T = ze^T$) that enumerates rooted labelled nonplanar trees.

(*c*) The case $\lambda = 3/2$ that appears in maps is the one that motivated the present paper, the law being precisely of the Airy type in this case. Equivalently, the estimates involve the stable law of index $\frac{3}{2}$. The singular exponent $\frac{3}{2}$ is generally expected in *unrooted* trees since there is a ratio of about n between the numbers of rooted and unrooted trees. The recent book of Kolchin [31] discusses the enumeration of forests of unrooted labelled trees by number of components: what is here at stake is the estimation of coefficients $[z^n]U(z)^k$ where $U(z)$ is the exponential generating function of unrooted trees, *i.e.*, $U = T - T^2/2$ where $T = ze^T$ is the Cayley tree function. Consequently, an Airy density is expected to surface in the asymptotic estimates: see Theorem 1.4.2 of [31] for an illustration. (Kolchin's method is based on characteristic functions and is equivalent to integrating along the circle of convergence rather than going *outside*.) Next, the "giant paper on the giant component" [29] analyses the random graph in its "critical" region where the (unrooted) tree components play an essential rôle. The analysis involves functions closely related to Airy functions. It is interesting to note that the proof of a major lemma, Lemma 3 of [29], does rely on a contour of the same type as ours. (The seven page proof in [29] is justified by the need there to develop uniform estimates valid in a wide region as well as to cope with a singular multiplier.) Finally, a similar situation is encountered in [18, p. 182–183] where the paper deals with the appearance of the first cycles in random graphs.

Combinatorial compositions. The results of Theorem 11 provide useful information on composition schemas of the form

$$M(z,u) = C(uH(z)),$$

provided C and H are algebraic-logarithmic in the sense above. Combinatorially, this represents a substitution between structures, $\mathcal{M} = \mathcal{C} \circ \mathcal{H}$, and the coefficient $[z^n u^k]M(z,u)$ counts the number of $\mathcal{M}$-structures of size n whose $\mathcal{C}$-core has size k. Then the probability distribution of core size X_n in $\mathcal{M}$-structures of size n is given by

$$\Pr(X_n = k) = \frac{[z^k]C(z)}{[z^n]C(H(z))}\,[z^n]H(z)^k.$$

The case where the schema is critical[7], in the sense that $H(r_H) = r_C$ with r_H, r_C the radii of convergence of H, C, follows as a direct consequence of Theorem 11. What comes out is the following informally stated general principle (details would closely mimic the statement of Theorem 11 and are omitted).

Theorem 12 (General composition schema)**.** *In a composition schema $C(uH(z))$ where H and C have singular exponents λ, λ' (with $\lambda' \leqslant \lambda$):*

[7]Noncritical cases follow from standard methods. In the subcritical case $H(r_H) < r_C$, core size is $O(1)$ with high probability and its law is directly induced from the initial coefficients of C. (This results from direct singularity analysis.) In the supercritical case $H(r_H) > r_C$ core size is typically about $O(n)$ and obeys a Gaussian law in the limit. (This results from standard singularity perturbation techniques as developed in [4, 23, 28].)

(i) for $0 < \lambda < 1$, the normalized core size X_n/n^λ is spread over $(0, +\infty)$ and it satisfies a local limit law whose density involves the stable law of index λ;

(ii) for $1 < \lambda < 2$, the distribution of X_n is bimodal and the "large" region $X_n = cn + xn^{1/\lambda}$ leads to a stable law of index λ;

(iii) for $2 < \lambda$, the standardized version of X_n admits a local limit law that is of Gaussian type.

Similar phenomena occur when $\lambda' > \lambda$, but with a greater preponderance of the "small" region.

Many instances have already appeared scattered in the literature. especially in connection with rooted trees. For instance, the Rayleigh law ($\lambda = \frac{1}{2}$) appears as the distribution of cyclic points in random mappings; see [13] for this fact and many other occurrences of this law. Naturally, the case $\lambda = 3/2$ present in maps is of the one that has motivated the present study.

Appendix B. The Airy distribution

In this appendix, we summarize a few properties of the Airy distribution, namely, integral representations, series expansions, and integral transforms.

(i) Integral representations. The Airy distribution appears first through local expansions of nearby saddle points (Section 2 and proof of Theorem 3), as

$$\mathcal{A}(x) = \frac{1}{i\pi} \int_{\infty e^{-i\theta}}^{\infty e^{i\theta}} \exp\left(\frac{1}{3}u^3 - xu^2\right) u\, du, \qquad \theta \in (\frac{\pi}{6}, \frac{\pi}{3}). \tag{68}$$

This form clearly shows its origin as an exponential-cubic approximation. In the context of singularity analysis (Section 4 and Appendix A), what arises is the integral representation

$$\mathcal{A}(x) = \frac{1}{2i\pi} \int_{\infty e^{-i\theta'}}^{\infty e^{i\theta'}} \exp\left(\frac{1}{3}t^{3/2} - xt\right) dt, \qquad \theta' \in (\frac{\pi}{3}, \frac{2\pi}{3}), \tag{69}$$

which is trivially equivalent to (68) via the change of variable $u = t^2$. A translation $u = v + x$ transforms the integral of (68) into

$$\mathcal{A}(x) = e^{-2x^3/3} \frac{1}{i\pi} \int_{\infty e^{-i\theta}}^{\infty e^{i\theta}} \exp\left(\frac{1}{3}v^3 - vx^2\right) (v + x)\, dx. \tag{70}$$

This last form is equivalent (modulo the rotation $v = -iw$) to the definition we gave (Definition 1) of the Airy distribution by way of the Airy function, itself defined by the integral representation (1). As asymptotic expansions of the Airy function at $\pm\infty$ have long been tabulated, one additionally obtains from the Airy connection the tail estimates expressed by (3).

(ii) Series expansions. The expression of the Airy distribution in terms of the Airy function is itself a series expansion in disguise. A direct expansion is obtained by starting from (69), expanding into power series the exponential $\exp(-xt)$, and integrating termwise. The process is the one also used in a general context in Appendix A. The net result is the form

$$\mathcal{A}(x) = \frac{1}{\pi x} \sum_{n \geqslant 1} (-x3^{2/3})^n \frac{\Gamma((2n+3)/3)}{n!} \sin(-2n\pi/3). \tag{71}$$

Naturally, this means that the Airy density is reducible to hypergeometric functions.

(*iii*) *Mellin transforms.* The Mellin transform of a function $f(x)$ that exists on $(0,+\infty)$ is classically defined as

$$f^\star(s) = \mathfrak{M}(f(x)\,;s) := \int_0^\infty f(x)x^{s-1}\,dx.$$

Knowledge of the Mellin transform (at s) of a probability density supported on $(0,+\infty)$ is thus equivalent to knowledge of a fractional moment (of order $s-1$) of the density. For the Airy distributions, we define separately

$$\mathcal{A}_+(x) := \text{if } x>0 \text{ then } \mathcal{A}(x) \text{ else } 0; \qquad \mathcal{A}_-(x) := \text{if } x<0 \text{ then } \mathcal{A}(-x) \text{ else } 0.$$

The corresponding Mellin transforms are then written as $\mathcal{A}_+^\star(s)$ and $\mathcal{A}_-^\star(s)$. In the case at hand, there are two possible approaches to the determination of the transform: one is based on the integral representations (68) or (69) and the general transform of multiplicative convolution integrals,

$$\mathfrak{M}\left(\int_\gamma a(u)b(xu)du\,;s\right) = b^\star(s)\int_\gamma a(u)u^{-s}\,du$$

(this results from an interchange of integrals; see [47, p. 151]); the other is based on the series expansion (71) and the general Mellin-Lindelöf-Ramanujan representation

$$\sum_{n=1}^\infty \phi(n)\frac{(-x)^n}{n!} = \frac{1}{2i\pi}\int_{-1/2-i\infty}^{-1/2+i\infty}\phi(-s)\Gamma(s)x^{-s}\,ds,$$

or, equivalently,

$$\phi(-s)\Gamma(s) = \mathfrak{M}\left(\sum_{n=1}^\infty \phi(n)\frac{(-x)^n}{n!}\,;s\right)$$

(this results from a residue calculation and from the Mellin inversion formula; see [27, Ch. XI]).

For the Airy distributions either method is applicable and one finds (after routine manipulations)

$$\mathcal{A}_+^\star(s) = 2\,3^{-\frac{2s+1}{3}}\frac{\Gamma(s)}{\Gamma\left(\frac{2s+1}{3}\right)}, \quad 0<\Re(s)<\infty \tag{72}$$

$$\mathcal{A}_-^\star(s) = 3^{-\frac{2s+1}{3}}\frac{\Gamma(s)}{\Gamma\left(\frac{2s+1}{3}\right)}\frac{1}{\cos\frac{\pi}{3}(s-1)}, \quad 0<\Re(s)<\frac{5}{2}. \tag{73}$$

In particular, one has $\mathcal{A}_+(1)=\frac{2}{3}$, $\mathcal{A}_-(1)=\frac{1}{3}$. This verifies that $\mathcal{A}(x)$ is a probability density and that two thirds of the probability mass are assigned to the positive region. Also, $\mathcal{A}_+(2)=\mathcal{A}_-(2)=3^{-2/3}/\Gamma(2/3)$, which implies that the mean of the Airy distribution equals 0. Generally, formulæ (72) and (73) can be used to evaluate explicitly any fractional moment of the Airy law, for instance,

$$\int_{-\infty}^\infty \sqrt{|x|}\mathcal{A}(x)\,dx = \frac{1}{6\sqrt{\pi}}\Gamma(\frac{2}{3})\left(3^{2/3}+3^{7/6}\right).$$

Appendix C. Conformality of $z(t)$ and coalescent saddles

In this section, we take $k=\alpha_0 n+\beta n$, with β fixed and the notations of Section 3 are used. We prove that there exists indeed a change of variable $z\to t$, with $\tau_d = \pm\xi$, that satisfies (43) and is a conformal mapping of the disc D onto a domain D_β. The strategy consists in constructing first a mapping $z\to t$ that is

continuous and one-to-one between D and some domain D_β, then checking that it is conformal.

C.1. **A one-to-one continuous mapping.** The mapping $z \to u = K(z)$ is continuous for $z \in D$ and so is the mapping $t \to u = f(t)$ for $t \in \mathbb{C}$. The problem is that they are not one-to-one. However we shall provide a partition of the whole complex plane $\mathbb{C} = \bigcup_{i=1}^{6} C_i$ such that each $f|_{C_i}$ is one-to-one, another partition $D = \bigcup_{i=1}^{6} D_i$ such that each restriction $K|_{D_i}$ is one-to-one, and such that $K(D_i) \subset f(C_i)$.

This will allow us to define for each i a continuous one-to-one mapping $z \to t$ from D_i onto $C_i' \subset C_i$; we shall choose the D_i so that it follows immediately that the resulting six mappings coherently define a one-to-one mapping of D onto a domain D_β.

Let $\mathcal{H}_+$, $\mathcal{H}_-$ and $\mathcal{H}_0$ denote respectively the half planes $\{u \mid \Im u \geqslant 0\}$, $\{u \mid \Im u \leqslant 0\}$ and imaginary u-axis. The partition of $\mathbb{C}$ is readily obtained by considering the inverse image of $\mathcal{H}_0$ by f, *i.e.*, the curve

$$\mathcal{C}_0 = \{t \mid \Im f(t) = 0\} = \mathbb{R} \cup \{t = x + iy \mid 3s^2 - 3x^2 + y^2\}.$$

The three smooth components of this curve partition the t-plane into six regions C_i, as defined for $\beta < 0$, $\beta = 0$ and $\beta > 0$ by Figure 15. More precisely we take each C_i to include its border, so that its image is $\mathcal{H}_+$ for $i = 1, 3, 5$ and $\mathcal{H}_-$ for $i = 2, 4, 6$. In particular each $C_i \cap C_j$ is either empty or a smooth segment of the curve $\mathcal{C}_0$.

In each of the two regions C_1, C_4, one easily verifies that $\Re f'(t)$ has a constant nonzero sign. In each of the other four regions, $\Im f'(t)$ has a constant nonzero sign. Hence in each region C_i, the mapping $t \to f(t)$ is one-to-one (and of course continuous).

The construction is exactly the same for the mapping $z \to K(z)$, except that the region of interest is restricted to D. From the technical point of view, one has to study the curve

$$\begin{aligned}\mathcal{D}_0 &= \{z \mid \Im K(z) = 0\} \\ &= \mathbb{R} \cup \{z \mid 2\arg((3-z)(1+z)^3/z) + 3\beta \arg(z(3-z)^2) = 0\},\end{aligned}$$

and prove that inside the disc D, it behaves qualitatively like C_0. This analysis is done in view of the derivative

$$K'(z) = (z - \tau)(z - \tau')\frac{3\beta + 2}{z(1+z)(3-z)}$$

that depends linearly on β. As illustrated by Figure 16 and 17 the landscape of $\Im K(z)$ leads to a partition D_i in agreement with the partition C_i of Figure 15.

Once this is done, the local mappings can be composed to give six local mapping $z \to t$. These local mappings are coherent since the local mappings are identical on the intersection $D_i \cap D_j$ and $C_i \cap C_j$. Thus, a continuous one-to-one mapping from D to a domain D_β has been defined and we let $z(t)$ be the inverse mapping.

C.2. **A study of $\dot{z}(t)$.** In order for the constructed mapping $z \to t$ to be conformal, it remains to check the necessary condition that $\dot{z}(t)$ is finite and nonzero. But, by differentiation of (43), one has

$$\dot{z}(t)K'(z) = -\left(t^2 - \xi^2\right), \tag{74}$$

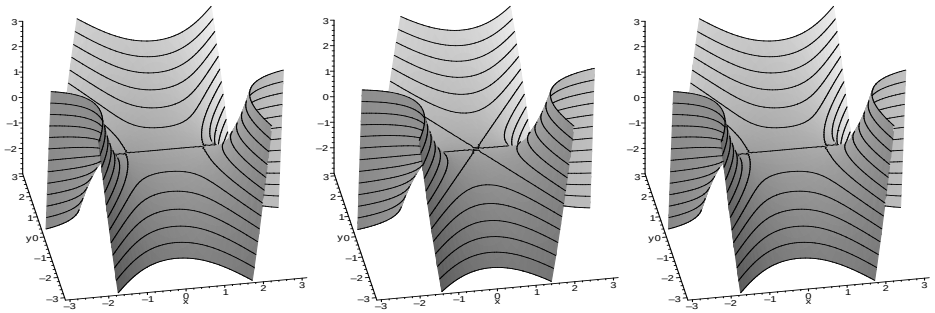

FIGURE 14. The landscape of $\Im f(t)$, for $\beta < 0$, $\beta = 0$ and $\beta > 0$.

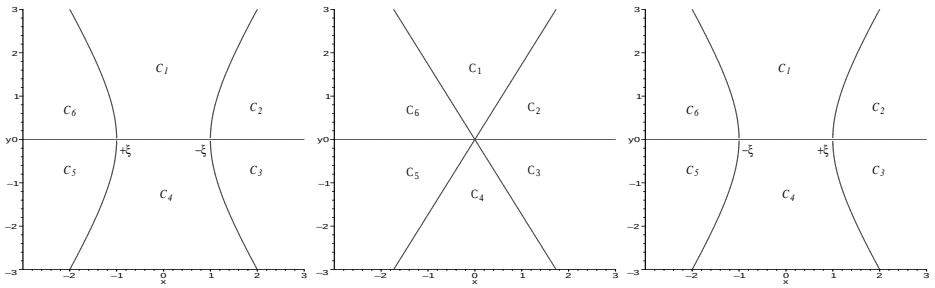

FIGURE 15. Partition of the t-plane, for $\beta < 0$, $\beta = 0$ and $\beta > 0$.

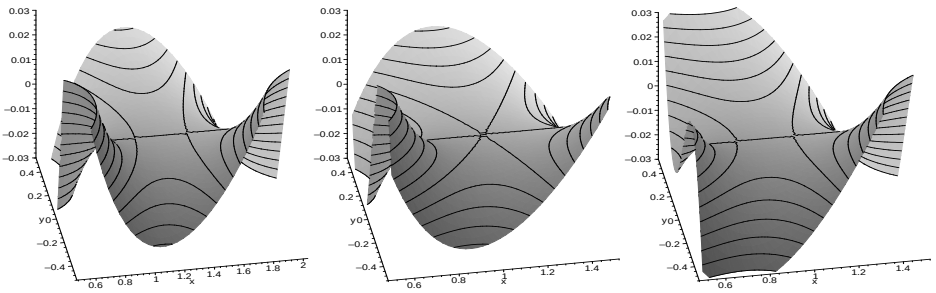

FIGURE 16. The landscape of $\Im K(z)$, for $\beta < 0$, $\beta = 0$ and $\beta > 0$.

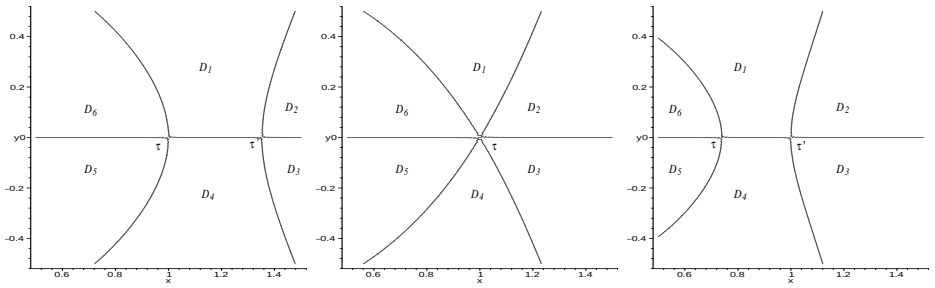

FIGURE 17. Partition of the z-plane, for $\beta < 0$, $\beta = 0$ and $\beta > 0$.

so that $\dot{z}(t)$ is seen to satisfy

$$\dot{z}(t) = \frac{t-\xi}{z-\tau}\frac{t+\xi}{z-\tau'}\frac{(3-z)(1+z)z}{2+3\beta}. \tag{75}$$

Hence in D, there may only be problems at $z=\tau$ and $z=\tau'$. But letting t go to ξ or $-\xi$ this provides

$$\dot{z}(\xi)^2 = \frac{-\xi}{\tau'-\tau}\frac{(3-\tau)(1+\tau)\tau}{2+3\beta} \quad \text{and} \quad \dot{z}(-\xi)^2 = \frac{\xi}{\tau'-\tau}\frac{(3-\tau')(1+\tau')\tau'}{2+3\beta}.$$

Finally the sign is seen to be positive by considering a point other than $\pm\xi$ on the real axis. This yields

$$\dot{z}(\xi) = \sqrt{\frac{4\xi}{3\beta}} \quad \text{and} \quad \dot{z}(-\xi) = \sqrt{\frac{4\xi}{3\beta}\frac{(1+3\beta)(1-3\beta/2)}{(1+3\beta/2)^3}}. \tag{76}$$

These values are involved in the computation of a_1.

Appendix D. Largest components (proof of Theorem 7)

Let us first prove Theorem 7 in the case of nonseparable cores of maps. Recall that $M_{n,k}$ is the number of maps of size n with a core of size k, and set the following notations: $M^*_{n,k}$ is the number of maps of size n with a largest component of size k; $B_{n,k}$ is the number of maps of size n with a core of size k that is not the largest component. Then, the following relation holds:

$$2nM_{n,k} = 2kM^*_{n,k} + 2nB_{n,k}. \tag{77}$$

This relation is proven in two steps. First of all, amongst the $2nM_{n,k}$ maps of size n with a core of size k and a secondary root, exactly $2nB_{n,k}$ have a core which is not the largest component. Second of all, the remaining maps have a core which is the largest component and, upon exchanging the rôle of the two roots, they are identified with the $2kM^*_{n,k}$ maps that have a largest component of size k and a secondary root chosen in the largest component.

The following lemma next allows us to dispose of the $B_{n,k}$ term.

Lemma 1. *Under the uniform distribution on maps with size n and core-size $k = \lfloor \alpha_0 n + x n^{2/3} \rfloor$ for some x, the core is almost surely the largest component.*

More precisely, there exists $A < 1$ such that

$$\Pr(X^*_n > X_n \mid X_n = k) = \frac{B_{n,k}}{M_{n,k}} = O(A^n),$$

with $k = \lfloor \alpha_0 n + x n^{2/3} \rfloor$, uniformly for x in a bounded interval.

Proof. Let $\mathfrak{m}$ be a map of size n with a core $\mathfrak{c}$ of size k and a largest component $\mathfrak{l}$ of size $h > k$. The largest component $\mathfrak{l}$ is contained in one of the pending submap $\mathfrak{n}$ in the core decomposition of $\mathfrak{m}$. Let $\mathfrak{m}'$ be obtained from $\mathfrak{m}$ by detaching $\mathfrak{n}$. Then $\mathfrak{m}$ can be uniquely reconstructed from $\mathfrak{m}'$, $\mathfrak{m}$ and the position in the core of $\mathfrak{m}'$ where $\mathfrak{n}$ is to be attached. The number $B_{n,k}$ of maps $\mathfrak{m}$ is thus bounded from above by the number of such triples: with ℓ representing the size of $\mathfrak{n}$,

$$B_{n,k} \le \sum_{k<h<\ell<n-k} M_{n-\ell,k} \cdot M^*_{\ell,h} \cdot 2k \ \le 2k \sum_{k<h<\ell<n-k} \frac{\ell}{h} M_{n-\ell,k} M_{\ell,h},$$

where the second inequality follows from (77). Hence the probability satisfies

$$\frac{B_{n,k}}{M_{n,k}} \leq 2k \sum_{k<h<\ell<n-k} \frac{\ell}{h} \frac{M_{n-\ell,k}}{M_{n-\ell}} \frac{M_{\ell,h}}{M_\ell} \frac{M_n}{M_{n,k}} \frac{M_\ell M_{n-\ell}}{M_n}$$

Theorem 5 allows us to bound the ratios: the rough upper bound $M_{\ell,h}/M_\ell = O(h^{-2/3})$ is valid for all ℓ, h; $M_{n,k}/M_n = \Theta(n^{-2/3})$ since $k = \alpha_0 n + x n^{2/3}$ with x bounded; finally $k/(n-\ell) \sim \frac{\alpha_0}{1-\alpha_0} > \alpha_0$, so that there exists $A_0 < 1$ such that $M_{n-\ell,k}/M_{n-\ell} = O(A_0^k)$. This ensures the existence of some $A_1 < 1$ such that

$$\frac{B_{n,k}}{M_{n,k}} \leq C_1 n \sum_{k<h<\ell<n-k} \frac{\ell}{h} \cdot A_0^k h^{-2/3} n^{2/3} \frac{n^{5/2}}{\ell^{5/2}(n-\ell)^{5/2}} \leq C_2 A_1^n,$$

hence the statement of the lemma. □

Finally, Lemma 1 and Relation (77) combine to yield

$$M^*_{n,k} = \frac{n}{k} M_{n,k} \left(1 + O(A^n)\right) = \frac{1}{\alpha_0} M_{n,k} \left(1 - \tfrac{x}{\alpha_0} n^{-1/3} + O(n^{-2/3})\right)$$

for $k = n/3 + x n^{2/3}$, uniformly for x in a bounded interval. Together with $\alpha_0 = p_\ell$, this concludes the proof of Theorem 7 for nonseparable components of maps.

The proof extends verbatim for all schemas with $\alpha_0 = p_\ell$. For the two remaining ones a difference arises from the fact that some edges are shared by different components (*e.g.*, the edges of separating 3-cycles get duplicated in the decomposition of triangulations into irreducible triangulations). The same difference surfaces in [7, 24] in the proof given there of our Equation (62). The adaptation given in [7, 24] of the general argument to the case of irreducible cores of triangulations and 3-connected cores of nonseparable maps works equally well in our case.

Acknowledgements. This work was supported in part by the IST Programme of the EU under contract number IST-1999-14186 (ALCOM-FT).

References

[1] Abramowitz, M., and Stegun, I. A. *Handbook of Mathematical Functions.* Dover, 1973. A reprint of the tenth National Bureau of Standards edition, 1964.

[2] Banderier, C., Flajolet, P., Schaeffer, G., and Soria, M. Planar maps and Airy phenomena. In *Automata, Languages, and Programming* (2000), E. W. U. Montanari, J. Rolim, Ed., no. 1853 in Lecture Notes in Computer Science, pp. 388–402. Proceedings of the 27th ICALP Conference, Geneva, July 2000.

[3] Bender, C. M., and Orszag, S. A. *Advanced mathematical methods for scientists and engineers. I.* Springer-Verlag, New York, 1999. Asymptotic methods and perturbation theory, Reprint of the 1978 original.

[4] Bender, E. A. Central and local limit theorems applied to asymptotic enumeration. *Journal of Combinatorial Theory 15* (1973), 91–111.

[5] Bender, E. A. Asymptotic methods in enumeration. *SIAM Review 16*, 4 (Oct. 1974), 485–515.

[6] Bender, E. A. Some unsolved problems in map enumeration. *Bull. Inst. Combin. Appl. 3* (1991), 51–56.

[7] Bender, E. A., Richmond, L. B., and Wormald, N. C. Largest 4-connected components of 3-connected planar triangulations. *Random Structures & Algorithms 7*, 4 (1995), 273–285.

[8] Bleistein, N., and Handelsman, R. A. *Asymptotic Expansions of Integrals.* Dover, New York, 1986. A reprint of the second Holt, Rinehart and Winston edition, 1975.

[9] Bollobás, B., Borgs, C., Chayes, J. T., Kim, J. H., and Wilson, D. B. The scaling window of the 2-SAT transition. Preprint, 1999. Available as document math.CO/9909031 at the Los Alamos archive `http://xxx.lanl.gov/form/`.

[10] Bousquet-Mélou, M., and Schaeffer, G. Enumeration of planar constellations. *Adv. in Appl. Math. 24*, 4 (2000), 337–368.
[11] Breiman, L. *Probability*. Society for Industrial and Applied Mathematics (SIAM), Philadelphia, PA, 1992. Corrected reprint of the 1968 original.
[12] De Bruijn, N. G. *Asymptotic Methods in Analysis*. Dover, 1981. A reprint of the third North Holland edition, 1970 (first edition, 1958).
[13] Drmota, M., and Soria, M. Images and preimages in random mappings. *SIAM Journal on Discrete Mathematics 10*, 2 (1997), 246–269.
[14] Duchon, P. Q-grammars and wall polyominoes. *Annals of Combinatorics 3* (1999), 311–321.
[15] Durrett, R. *Probability: theory and examples*, second ed. Duxbury Press, Belmont, CA, 1996.
[16] Feller, W. *An introduction to probability theory and its applications. Vol. II.*, second ed. John Wiley & Sons Inc., New York, 1971.
[17] Flajolet, P. Singularity analysis and asymptotics of Bernoulli sums. *Theoretical Computer Science 215*, 1-2 (1999), 371–381.
[18] Flajolet, P., Knuth, D. E., and Pittel, B. The first cycles in an evolving graph. *Discrete Mathematics 75* (1989), 167–215.
[19] Flajolet, P., and Louchard, G. Analytic variations on the Airy distribution. Technical Report TR-01-15, Alcom-FT Project, 2001. (To appear in *Algorithmica*, Special Issue on Analysis of Algorithms 2002; 16p.).
[20] Flajolet, P., and Odlyzko, A. M. Singularity analysis of generating functions. *SIAM Journal on Applied Mathematics 3*, 2 (1990), 216–240.
[21] Flajolet, P., Poblete, P., and Viola, A. On the analysis of linear probing hashing. *Algorithmica 22*, 4 (1998), 490–515.
[22] Flajolet, P., Salvy, B., and Schaeffer, G. Airy phenomena and analytic combinatorics of connected graphs. Research report, Institut National de Recherche en Informatique et en Automatique, 2001. In preparation.
[23] Flajolet, P., and Soria, M. General combinatorial schemas: Gaussian limit distributions and exponential tails. *Discrete Mathematics 114* (1993), 159–180.
[24] Gao, Z., and Wormald, N. C. The size of the largest components in random planar maps. *SIAM J. Discrete Math. 12*, 2 (1999), 217–228 (electronic).
[25] Gardy, D. Some results on the asymptotic behaviour of coefficients of large powers of functions. *Discrete Mathematics 139*, 1-3 (1995), 189–217.
[26] Goulden, I. P., and Jackson, D. M. *Combinatorial Enumeration*. John Wiley, New York, 1983.
[27] Hardy, G. H. *Ramanujan: Twelve Lectures on Subjects Suggested by his Life and Work*, third ed. Chelsea Publishing Company, New-York, 1978. Reprinted and Corrected from the First Edition, Cambridge, 1940.
[28] Hwang, H.-K. *Théorèmes limites pour les structures combinatoires et les fonctions arithmetiques*. PhD thesis, École Polytechnique, 1994.
[29] Janson, S., Knuth, D. E., Łuczak, T., and Pittel, B. The birth of the giant component. *Random Structures & Algorithms 4*, 3 (1993), 233–358.
[30] Knuth, D. E. Linear probing and graphs. *Algorithmica 22*, 4 (1998), 561–568.
[31] Kolchin, V. F. *Random Graphs*, vol. 53 of *Encyclopedia of Mathematics and its Applications*. Cambridge University Press, Cambridge, U.K., 1999.
[32] Liskovets, V. A. A pattern of asymptotic vertex valency distributions in planar maps. *J. Combin. Theory Ser. B 75*, 1 (1999), 116–133.
[33] Louchard, G. The Brownian excursion: a numerical analysis. *Computers and Mathematics with Applications 10*, 6 (1984), 413–417.
[34] Meir, A., and Moon, J. W. On the altitude of nodes in random trees. *Canadian Journal of Mathematics 30* (1978), 997–1015.
[35] Odlyzko, A. M. Asymptotic enumeration methods. In *Handbook of Combinatorics*, R. Graham, M. Grötschel, and L. Lovász, Eds., vol. II. Elsevier, Amsterdam, 1995, pp. 1063–1229.
[36] Pemantle, R. Generating functions with high-order poles are nearly polynomial. In *Mathematics and computer science (Versailles, 2000)*. Birkhäuser, Basel, 2000, pp. 305–321.
[37] Prellberg, T. Uniform q-series asymptotics for staircase polygons. *Journal of Physics A: Math. Gen. 28* (1995), 1289–1304.

[38] Richmond, L. B., and Wormald, N. C. Almost all maps are asymmetric. *Journal of Combinatorial Theory. Series B 63*, 1 (1995), 1–7.
[39] Schaeffer, G. *Conjugaison d'arbres et cartes combinatoires aléatoires*. PhD thesis, Université Bordeaux I, 1998.
[40] Schaeffer, G. Random sampling of large planar maps and convex polyhedra. In *Proceedings of the thirty-first annual ACM symposium on theory of computing (STOC'99)* (Atlanta, Georgia, 1999), ACM press, pp. 760–769.
[41] Soria-Cousineau, M. *Méthodes d'analyse pour les constructions combinatoires et les algorithmes*. Doctorate in sciences, Université de Paris–Sud, Orsay, 1990.
[42] Takacs, L. A Bernoulli excursion and its various applications. *Advances in Applied Probability 23* (1991), 557–585.
[43] Tutte, W. T. A census of planar maps. *Canad. J. Math. 15* (1963), 249–271.
[44] Tutte, W. T. Planar enumeration. In *Graph theory and combinatorics (Cambridge, 1983)*. Academic Press, London, 1984, pp. 315–319.
[45] Watson, G. N. *A Treatise on the Theory of Bessel Functions*. Cambridge University Press, 1980.
[46] Whittaker, E. T., and Watson, G. N. *A Course of Modern Analysis*, fourth ed. Cambridge University Press, 1927. Reprinted 1973.
[47] Wong, R. *Asymptotic Approximations of Integrals*. Academic Press, 1989.
[48] Zolotarev, V. M. *One-dimensional stable distributions*. American Mathematical Society, Providence, RI, 1986. Translated from the Russian by H. H. McFaden, Translation edited by Ben Silver.

C.B.: Algorithms Project, INRIA, Rocquencourt, 78150 Le Chesnay (France)
E-mail address: Cyril.Banderier@inria.fr, http://algo.inria.fr/banderier

P.F.: Algorithms Project, INRIA, Rocquencourt, 78150 Le Chesnay (France)
E-mail address: Philippe.Flajolet@inria.fr, http://algo.inria.fr/flajolet

G.S.: Loria, CNRS, Campus sciences, B.P. 239, 54506 Vandœuvre-lès-Nancy (France)
E-mail address: Gilles.Schaeffer@loria.fr, http://www.loria.fr/~schaeffe

M.S.: Lip6, Université Paris 6, 8 rue du Capitaine Scott, 75005 Paris (France).
E-mail address: Michele.Soria@lip6.fr, http://algo.inria.fr/soria